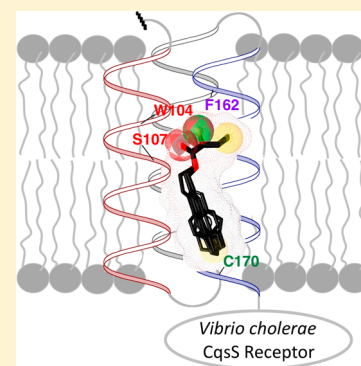


Role of the CAI-1 Fatty Acid Tail in the *Vibrio cholerae* Quorum Sensing ResponseLark J. Perez,^{†,||} Wai-Leung Ng,^{‡,⊥} Paul Marano,[†] Karolina Brook,[†] Bonnie L. Bassler,^{‡,§} and Martin F. Semmelhack^{*,†}[†]Department of Chemistry and [‡]Department of Molecular Biology, Princeton University, Princeton, New Jersey 08544, United States[§]Howard Hughes Medical Institute, Chevy Chase, Maryland 20815, United States

S Supporting Information

ABSTRACT: Quorum sensing is a mechanism of chemical communication among bacteria that enables collective behaviors. In *V. cholerae*, the etiological agent of the disease cholera, quorum sensing controls group behaviors including virulence factor production and biofilm formation. The major *V. cholerae* quorum-sensing system consists of the extracellular signal molecule called CAI-1 and its cognate membrane bound receptor called CqsS. Here, the ligand binding activity of CqsS is probed with structural analogues of the natural signal. Enabled by our discovery of a structurally simplified analogue of CAI-1, we prepared and analyzed a focused library. The molecules were designed to probe the effects of conformational and structural changes along the length of the fatty acid tail of CAI-1. Our results, combined with pharmacophore modeling, suggest a molecular basis for signal molecule recognition and receptor fidelity with respect to the fatty acid tail portion of CAI-1. These efforts provide novel probes to enhance discovery of antivirulence agents for the treatment of *V. cholerae*.



1. INTRODUCTION

Many bacteria control collective behaviors using a cell-to-cell communication process called quorum sensing (QS).^{1,2} They sense cell population density through the production, release, and detection of extracellular signal molecules termed auto-inducers (AIs). The concentration of AIs grows in proportion to the cell population density; when a threshold AI concentration is achieved, the bacteria initiate a group-wide response that promotes induction and/or repression of target genes. Community-wide synchronization of gene expression results in behaviors that are effective only when undertaken simultaneously by large groups of cells. QS-controlled functions include virulence factor production, bioluminescence, biofilm formation, sporulation, and antibiotic synthesis.^{3–5}

In the human pathogen *V. cholerae*, QS is mediated by two parallel phospho-relay systems.⁶ One system, which is the focus of this study, employs the membrane-bound receptor CqsS to detect two related AI molecules, CAI-1 (1, (S)-3-hydroxytridecan-4-one)⁷ and Ea-CAI-1 (2, 3-aminotridec-2-en-4-one)⁸ (Figure 1c). Ea-CAI-1 is produced by the aminotransferase enzyme CqsA and is subsequently converted to CAI-1.⁹ Under conditions in which signal molecule concentration is below the threshold for detection, such as at low cell density, CqsS functions as a kinase, phosphorylating the response regulator LuxO. The phosphorylation of LuxO results in the expression of a regulon of low cell density genes, including those required for virulence factor production and biofilm formation. At high cell density, when CAI-1 accumulates to an appreciable level, binding of the ligand to CqsS inhibits its kinase activity, enabling its phosphatase activity to predominate. As a

consequence, phosphate flow in the circuit is reversed, leading to dephosphorylation and inactivation of LuxO; this initiates the high cell density QS gene expression program. Under this condition, production of virulence factors and biofilm formation are repressed. By contrast, activation of the expression of a protease gene occurs, and this protease facilitates the exit of *V. cholerae* from its host.¹⁰

CAI-1 and Ea-CAI-1 each contain a three-carbon unit derived from (S)-adenosyl methionine (SAM) (highlighted in red, Figure 2) attached to an acyl tail.⁹ Likewise, *Legionella pneumophila* employs an analogue of CAI-1 (LAI-1, 3-hydroxypentadecan-4-one) with a C-12 acyl tail,¹¹ and *Vibrio harveyi* employs an analogue of Ea-CAI-1 (C8-Ea-CAI-1, 3-aminoundec-2-en-4-one) with a C-8 acyl tail.⁸ On the basis of these discoveries, we propose that while the conserved polar portion (in red) of this family of signaling molecules certainly plays a role in receptor binding, the variable acyl tail defines receptor specificity and is required to maintain signaling fidelity. This analysis has a strong analogy in the widely studied QS acylhomoserine lactone AIs (AHLs).² The AHLs similarly comprise a structurally conserved polar fragment, the homoserine lactone, derived from SAM, and a variable fragment, the acyl tail, derived from fatty acid biosynthesis (Figure 2).

Bacterial histidine kinases, including CqsS, are ubiquitous, and they relay extracellular sensory information into cells. These so-called two-component sensors generally have

Received: June 28, 2012

Published: October 23, 2012

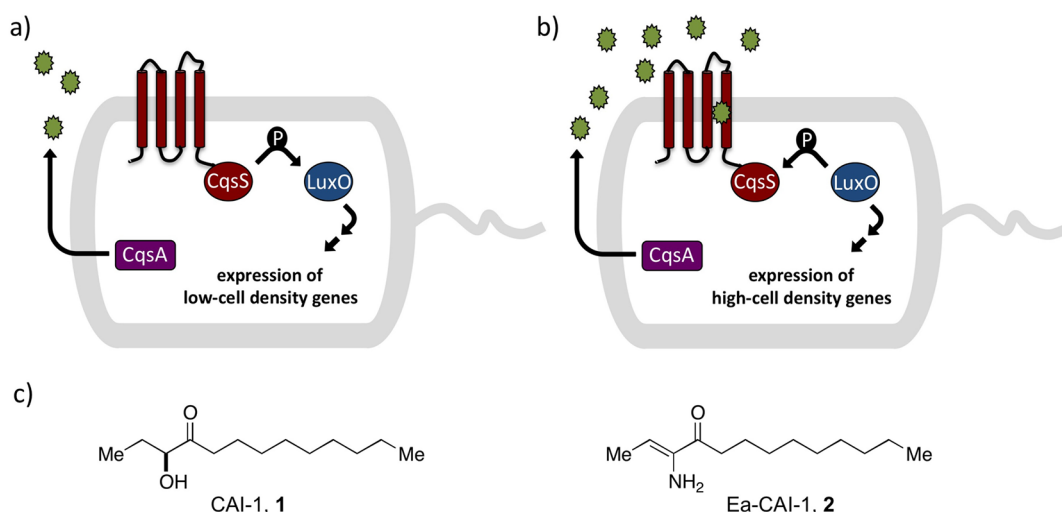


Figure 1. QS in *Vibrio cholerae*. (a) The CAI-1 AI (green circles) is produced by the CqsA synthase. Under conditions of low CAI-1 concentration, the cognate receptor CqsS acts as a kinase and transfers phosphate to LuxO, which leads to the expression of genes underpinning individual behaviors. (b) At high CAI-1 concentrations, CqsS binds CAI-1, and this converts CqsS from a kinase to a phosphatase. LuxO is dephosphorylated, which leads to the expression of genes required for group behaviors. (c) Native CAI-1 QS molecules in *V. cholerae*.

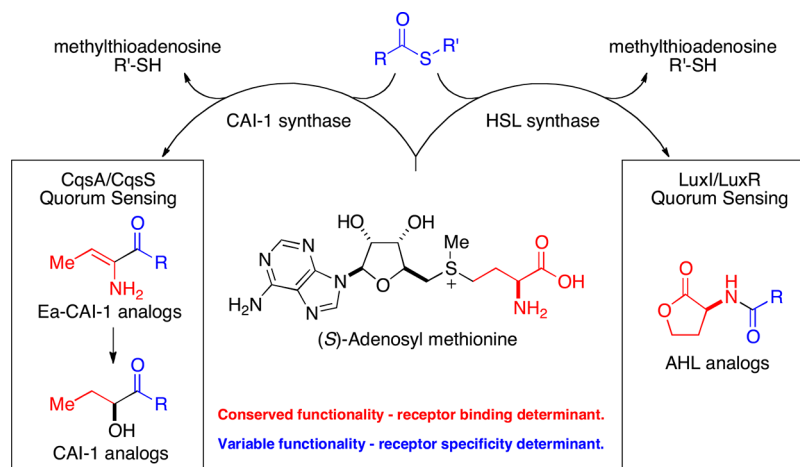


Figure 2. Simplified analysis of the structural features of the CAI-1 family of QS signal molecules. An equivalent of SAM (3) is incorporated into CAI-1, providing the structurally conserved portion of the final molecules (highlighted in red), along with an equivalent of a fatty acid in the form of a fatty acid thioester that provides the structurally variable portion of the signaling molecules (highlighted in blue) ($\text{RC}=\text{O}$ = fatty acid; R' = CoA or ACP).

complicated membrane-spanning domains, which has made structural analysis difficult. In the absence of detailed structural information, chemical genetics approaches can provide useful information about ligand–receptor interactions enabling the design and optimization of small molecule agonists and antagonists that serve as useful probes of signal transduction.

To define the roles of different structural features of *V. cholerae* CAI-1 in signal recognition and specificity, we previously examined three distinct chemical features of this ligand: (a) the ethyl side chain, (b) the 3-heteroatom substituent, and (c) the chain length of the acyl tail.¹² The structure–activity relationships can be summarized as follows: (a) the introduction of phenyl substitution in the ethyl side chain results in molecules that behave as antagonists; (b) the 3-heteroatom position is important for agonist activity with 3-OH or 3-NH₂ substitution being optimal; (c) the receptor is sensitive to changes in the chain length of the fatty acid tail with a C-9 or C-10 acyl tail being most potent.

We identified distinct amino acid residues in the CqsS transmembrane region that play corresponding roles in the recognition of each of these three structural features (Figure 3a).¹³ In summary, (a) F162 recognizes changes in the ethyl side chain, (b) W104 and S107 dictate the receptor's response to alterations at the 3-heteroatom position, and (c) C170 controls the receptor response to variations in the length of the acyl tail. These studies presumably reveal the location of the ligand binding pocket in the CqsS receptor as well as the constraints on allowable ligand alterations.

Here we expand our understanding of the SAR of CAI-1 with a focus on the effect of conformational and structural changes along the length of the fatty acid tail (library C in Figure 3a). As detailed below, the synthesis of a focused library of analogues was facilitated by the discovery that replacing the keto unit in CAI-1 with an ester group maintains full activity. These efforts provide a foundation for understanding signaling molecule specificity in the *V. cholerae* CqsS receptor and provide novel structures to serve as probes of this signaling circuit.

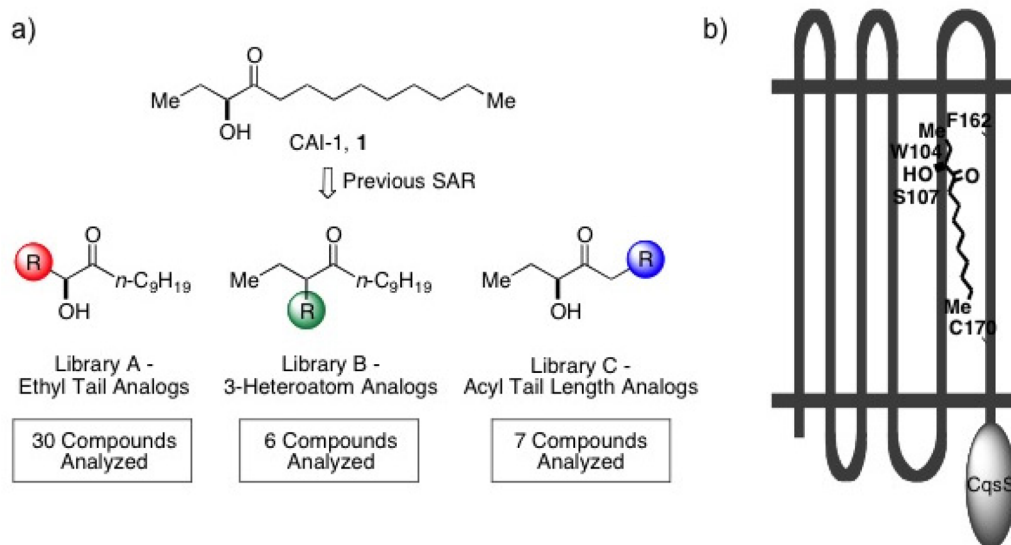


Figure 3. (a) SAR targeting three structural features of the CAI-1 signaling molecule. (b) Chemical–genetic analysis of CqsS enabling localization of the putative ligand binding pocket and identification of specific amino acid binding determinants.

2. RESULTS AND DISCUSSION

2.1. Assay Methods and Analysis. To quantify the induction of QS activity in *V. cholerae*, each of the CAI-1 analogues was added in triplicate to *V. cholerae* MM920 ($\Delta cqsA$, $\Delta luxQ$, pBB1 (a plasmid harboring the *V. harveyi luxCDABE* operon)) at increasing concentrations (typically using a 4-fold dilution series), and the light output from the heterologous luciferase reporter was monitored using a scintillation counter.¹⁴ Two parameters are described: (a) the EC_{50} values for activation of the QS response and (b) the maximum level of activation compared to the native signal CAI-1 as 100%. Percent response does not necessarily correlate with EC_{50} , as can be observed in Tables 1 and 3–6. Presumably this occurs because changes in the structure of the ligand or in the structure of the receptor binding site can alter the balance between kinase and phosphatase activities.¹²

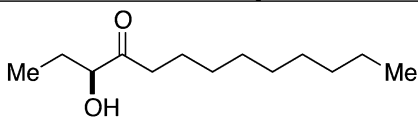
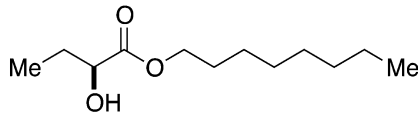
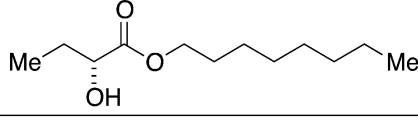
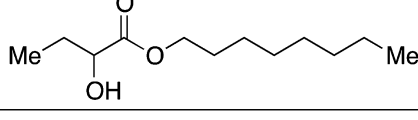
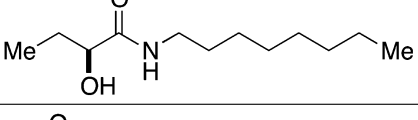
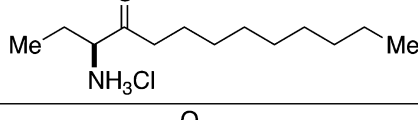
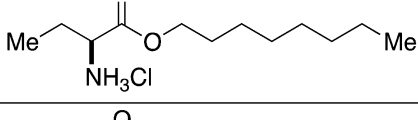
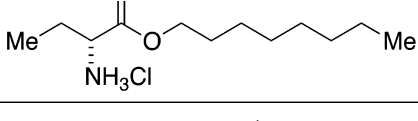
2.2. Design and Evaluation of Heterosubstitution in the Alkyl Tail: CAI-1 Ester and Amide Derivatives. An attractive approach for the preparation of a library differing in the alkyl tail involves the introduction of a heteroatom connector between the hydroxyketone portion and the alkyl tail (7–10, 12, 13, Table 1). These molecules were prepared by conventional methods of solution-phase synthesis (Scheme 1 (4 \rightarrow 6) and Supporting Information) and assayed for their biological activity (Table 1). The amide 10 displayed diminished activity in terms of its EC_{50} value (EC_{50} = 1500 nM) and maximal activity (81% of CAI-1 maximal response). The lower activity of the amide analogue compared to the parent CAI-1 ketone may be due to the geometrical constraints imposed by the amide functionality or due to unfavorable electronic interactions with the polarized amide structure. However we were pleased to find that ester analogue 7 closely maintained the activity profile of native CAI-1 in terms of EC_{50} (7, EC_{50} = 24 nM; CAI-1 (1) EC_{50} = 38 nM) and maximal induction of the QS response (7 = 106% response). The stereochemistry of the analogue plays a role in its potency, with the (*S*)-C8-ester-CAI-1 (7) displaying a 28-fold lower EC_{50} than the corresponding (*R*)-C8-ester-CAI-1 analogue (8). Both analogues were found to be capable of fully activating the QS response, and the racemate (9) showed intermediate activity

and full activation, as expected. Similar to previous observations, changing the 3-hydroxy substituent to amino (11–13) resulted in a potent QS agonist (EC_{50} of 30–33 nM; 107–108% response). To assess if these esters were serving as prodrugs,^{23,24} we assayed the activity of the alcohol tail of 9 (1-octanol) and 2-hydroxybutyric acid and found that these molecules show no QS activity up to 50 000 nM. Accordingly, for the systematic evaluation of tail structure, we have employed racemic mixtures of the 3-hydroxy ester derivatives.

2.3. Refinement of the Synthesis of Ester Analogues. Building on the discovery that the presence of an oxygen linker in the acyl tail (CAI-1 ester analogue 9) provides activity comparable to the native α -hydroxyl ketone signal, we prepared a larger library of CAI-1 ester analogues using an efficient one-step transesterification reaction of ethyl 2-hydroxybutyrate with a series of structurally diverse alcohols employing N-heterocyclic carbenes as catalysts.¹⁵ We optimized this reaction by varying the carbene catalyst, reaction time, and solvent (see Supporting Information). Catalyst 15 (10 mol %) was generally effective for the selective coupling of a series of primary alcohol tails with unprotected racemic ethyl 2-hydroxybutyrate (14, Scheme 2). Notably, under none of the conditions examined did we detect the formation of the undesired product involving esterification of the secondary alcohol on ethyl 2-hydroxybutyrate.^{16,17} By use of this methodology, four focused libraries of racemic CAI-1 esters were prepared by introducing (a) varying tail length, (b) ether substitution along the tail, (c) unsaturation in the tail, and (d) cycloalkyl and arene units in the tail (Tables 2–5).

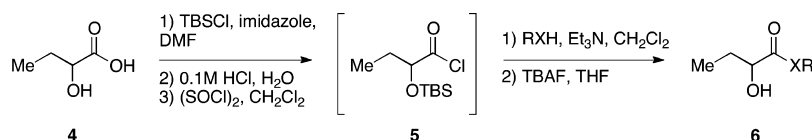
2.4. CAI-1 Ester Acyl Tail Length Analogues. The simple saturated CAI-1 ester analogues display a pattern of biological activity comparable to the previously reported series of CAI-1 tail length analogues (Table 2).¹² Specifically, the removal of a single methylene group from the saturated ester tail reduces the activity of analogue 19 2-fold compared to the racemic ester 9. In contrast, the addition of a single methylene as in 20 results in a 2-fold enhancement in the EC_{50} of the analogue (9, EC_{50} = 180 nM; 20, EC_{50} = 73 nM), whereas the addition of a single methylene in the hydroxy ketone series of molecules was previously reported to result in a 5-fold decrease

Table 1. Simple Ester and Amide CAI-1 Analogues

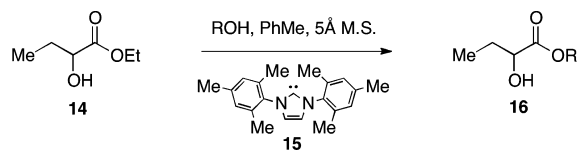
Entry	Compound	EC ₅₀ (nM) ^a	% Response ^b
1	 (S)-CAI-1, 1	38±3	100±4
2	 7	24±2	106±15
3	 8	670±240	94±35
4	 9	180±170	108±4
5	 10	1,500±220	81±11
6	 (S)-Am-CAI-1, 11	28±2	106±4
7	 12	30±2	108±3
8	 13	33±2	107±3

^aValues were determined using a light-based CqsS agonist bioassay (see Supporting Information). All EC₅₀ values are the mean of triplicate analyses with the range defining the 95% confidence interval. ^bPercent maximal bioluminescence with respect to CAI-1, which is set at 100%. The range defines the 95% confidence interval.

Scheme 1. Initial Synthesis of Structurally Simplified CAI-1 Analogues



Scheme 2. Second-Generation Synthesis of CAI-1 Ester Analogues

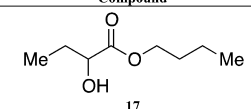
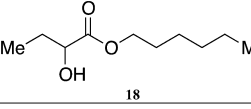
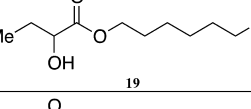
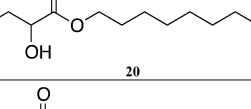
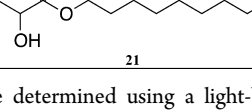


in EC₅₀.¹² The precise chain lengths in the ester series are not exactly the same as in the alkyl series: the C–O bond length (~1.35 Å) in an ester is less than the typical C–C bond length (1.54 Å); the 10-atom acyl chain in ester **9** is slightly shorter than the 10-carbon acyl chain in **1**. This feature may help rationalize why in the ester analogue the *addition* of a

methylene unit has a beneficial impact on analogue activity (2-fold decrease in EC₅₀) whereas the *removal* of a methylene group results in lower activity (4-fold increase in EC₅₀). The addition or removal of two methylene units (**21** and **18**) results in a greater than 4-fold decrease in activity from **9**, along with a decrease in the maximal % response (entries 2 and 5, Table 2). The removal of four methylene units (**17**) results in the nearly complete loss of QS activity.

As summarized in Figure 4, the SAR presented here closely mirrors that in our previous report involving a series of α -hydroxy ketone acyl tail length analogues. These data support our proposal that the α -hydroxy ester motif is a suitable framework for further exploration of the influence of tail structure on the activation of the CqsS receptor.

Table 2. CAI-1 Ester Chain-Length Analogues

Entry	Compound	EC ₅₀ (nM) ^a	% Response ^b
1		>50000	23 ^c
2		1,000±160	84±27
3		350±59	104±9
4		73±12	92±26
5		720±270	74±9

^aValues were determined using a light-based CqsS agonist bioassay (see Supporting Information). All EC₅₀ values are the mean of triplicate analyses with the range defining the 95% confidence interval. ^bPercent maximal bioluminescence with respect to CAI-1, which is set at 100%. The range defines the 95% confidence interval. ^cThe maximal % response at the maximum concentration tested (50 000 nM).

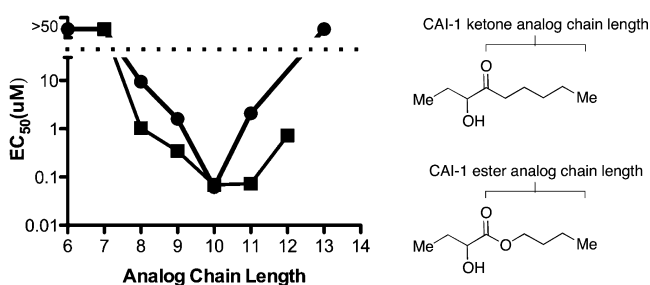


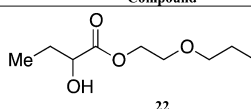
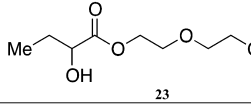
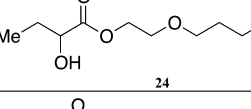
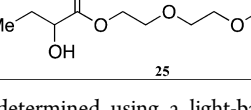
Figure 4. Comparison of EC₅₀ values as a function of acyl tail length for CAI-1 analogues: CAI-1 ketone acyl tail chain length EC₅₀ values (●)^b and CAI-1 ester chain length analogue EC₅₀ values (■).

2.5. CAI-1 Ester Analogues with Ether Substitution.

The highly lipophilic nature of the native CAI-1 and existing analogues may limit application as chemical probes in complex systems (e.g., in an animal host). In an effort to uncover effective agonists with polar functionality in the tail, we prepared a series of linear CAI-1 esters containing oxygen atoms at various positions along the ester tail. In general, the incorporation of the ether functionality results in the loss of biological activity (Table 3). A single additional oxygen atom in the CAI-1 ester tail, as in **22** and **24** results in a >13-fold decrease in activity from the C8-ester-CAI-1 (**9**); however, at sufficient concentration, these analogues did induce the maximal QS response (Table 3, entries 1 and 3). The diethylene glycol derived analogue, **23**, displays only minimal QS activity at 50 000 nM. Interestingly, however, the triethylene glycol derived analogue, **25**, stimulated the maximal QS response, although at relatively high concentrations (EC₅₀ = 10 000 nM).

2.6. Unsaturated CAI-1 Ester Analogues. A series of CAI-1 esters was prepared bearing units of unsaturation,

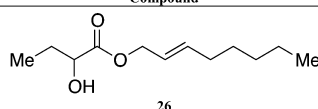
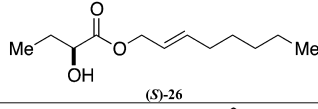
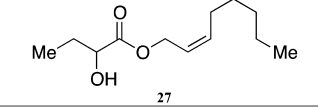
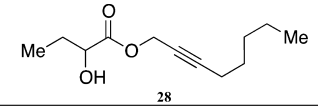
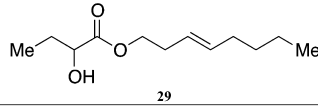
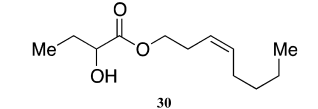
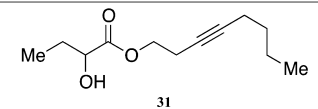
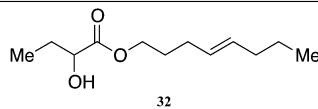
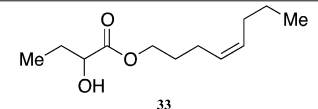
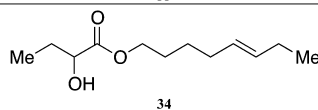
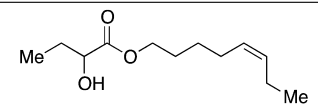
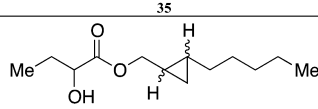
Table 3. Polar CAI-1 Ester Analogues

Entry	Compound	EC ₅₀ (nM) ^a	% Response ^b
1		4,400±450	96±8
2		>50,000	31 ^c
3		2,400±300	91±9
4		10,000±1,800	95±15

^aValues determined using a light-based CqsS agonist bioassay (see Supporting Information). All EC₅₀ values are the mean of triplicate analyses with the range defining the 95% confidence interval. ^bPercent maximal bioluminescence with respect to CAI-1, which is set at 100%. The range defines the 95% confidence interval. ^cThe maximal % response at the maximum concentration tested (50 000 nM).

including (*E*)- and (*Z*)-olefin isomers and alkynes, at specific positions along the alkyl tail portion. We expected these derivatives would clarify whether a linear (*E*-alkene or alkyne) or bent conformation (*Z*-alkene) of the tail is preferred. With one exception, full activation of the receptor was observed, but the EC₅₀ values varied as a function of both the configuration and position of the alkene unit (Table 4). The introduction of an (*E*)-alkene at the 2-position (2-(*E*)-ester-CAI-1, **26**) provided an analogue that was 3-fold more active than the fully saturated ester, **9** (Table 4, entry 1). In contrast, the presence of a (*Z*)-alkene at the 2-position (**27**, entry 2) led to an analogue that is almost 4-fold less active than C8-ester-CAI-1 (**9**). With an alkene in the 3-position, both the (*E*)- and (*Z*)-isomers displayed similarly diminished activity (4-fold lower EC₅₀ than **9**) (entries 4 and 5, respectively). Interestingly, in the 4-position, while the (*E*)-alkene (**32**, entry 7) was comparable in activity to the saturated C8-ester-CAI-1 with a 1.5-fold higher EC₅₀, the (*Z*)-isomer displayed significantly diminished activity (10-fold less active), similar to the 2-unsaturated alkenes, **23** and **24**. The 5-alkene isomers **34** and **35** again showed lower activity for both (*E*)- and (*Z*)-olefin isomers, analogous to the 3-unsaturated analogues **29** and **30**. The analogues bearing an alkyne at either the 2- or 3-position displayed diminished activity with the 3-isomer activating only 77% of the maximum response (entries 3 and 6). The 2-*trans*-cyclopropyl ester analogue **33** was also diminished in activity, almost 7 times less active than **9** (entry 11). Overall, the (*Z*)-alkene isomers (**27**, **30**, **33**, and **35**) all show diminished activity compared to the simple ester analogue **9** by a factor of 3 or more. In contrast, the (*E*)-alkene containing analogues display activities that are highly dependent on the position of the olefin, with the 2-(*E*) and 4-(*E*) analogues (**26** and **32**) exhibiting the greatest activity. Among this series of analogues that possess single points of conformational restriction along the length of the acyl tail portion of CAI-1, the 2-(*E*) analogue **26** uniquely displays enhanced potency compared to the fully saturated analogue, suggesting that the presence of a linear conformation of the alkyl tail proximal to the ester is favorable for binding. However, this effect is not simply conformational,

Table 4. Unsaturated CAI-1 Ester Analogues

Entry	Compound	EC ₅₀ (nM) ^a	% Response ^b
1	 26	54±8	98±9
1a	 (S)-26	39±5	99±13
2	 27	710±120	90±7
3	 28	550±86	104±8
4	 29	770±110	97±6
5	 30	780±130	100±10
6	 31	2,000±670	76±34
7	 32	270±33	103±5
8	 33	1,800±380	95±13
9	 34	830±100	101±6
10	 35	570±110	98±11
11	 36	1,200±600	98±21

^aValues determined using a light-based CqsS agonist bioassay (see Supporting Information). All EC₅₀ values are the mean of triplicate analyses with the range defining the 95% confidence interval. ^bPercent maximal bioluminescence with respect to CAI-1, which is set at 100%. The range defines the 95% confidence interval.

as the 2-*trans*-cyclopropyl analogue 36 displays diminished activity. As was observed in the series of saturated esters (7–9) the (*S*)-isomer of the most potent compound from this series (*S*)-26 (entry 1a) displays a lower EC₅₀ value than 26 (entry 1).

2.7. CAI-1 Ester Analogues with Cyclohexane or Benzene Units Incorporated in the Tail. We prepared a series of CAI-1 esters containing a cyclohexane or benzene unit at different positions of the CAI-1 ester tail. We anticipated that this series of analogues would provide information about the

steric demands of the binding pocket for the tail, as well as evidence regarding whether linear or bent conformations are favored.

One series of analogues bears substitution at the terminus of the ester tail, linked to the α -hydroxy ester headgroup by a three-, four-, or five-carbon chain (34–38). The activity of these analogues varies as a function of both the linker length and the terminating functionality (Table 5). The analogue bearing a five-carbon linker and a terminal phenyl substituent (38, entry 2) displayed the maximal response with an EC₅₀ of 110 nM. In contrast, the one-carbon shorter analogue bearing a terminal phenyl group (37) was diminished in activity (EC₅₀ = 1100 nM) and elicited a response of only 59% of the maximum value.

The saturated versions of these analogues, bearing a terminal cyclohexyl group, were universally more potent than the corresponding analogues bearing a terminal phenyl substituent. The analogue with a terminal cyclohexyl group and a four-carbon linker (40, entry 4) was the most potent in this series with an EC₅₀ of 84 nM, 2-fold more active than the simple ester 9. The analogues containing a one-carbon shorter linker (39) or a one-carbon longer linker (41) displayed EC₅₀ values of 310 and 190 nM, respectively.

Inserting a benzene ring into the alkyl chain with a linear 1,4-substitution pattern led to a series of active agonists. Two examples with equivalent overall chain length, 42 and 47, displayed equal activity (190 nM), and both achieved the maximal QS response (entries 6 and 11). The related structure with one additional methylene group in the chain (45) was less active (680 nM, entry 9). Introducing a nonlinear conformational restriction into the acyl tail of these analogues in the form of the 1,3-substituted aryl units, as in analogues 43, 46, and 48, resulted in a strong diminution in activity, with EC₅₀ values that were >9-fold lower than that of the parent C8-ester-CAI-1, 9. More dramatically, the 1,2-disubstituted phenyl analogues 44 and 49 showed very weak responses even at high concentrations (50 000 nM). These data suggest a binding pocket for the CAI-1 acyl tail that is somewhat permissive of greater steric demands (incorporation of the phenyl and cyclohexyl rings) but appears to strongly favor an overall linear conformation of the tail. In these analogues, the aromatic ring appears to contribute to activity beyond simply defining the linear substitution pattern, as other analogues displaying an overall linear orientation of the alkyl tail were found to be less active (compare 42 with 28 (Table 4)). Consistent with our expectations, the (*S*)-isomers of two of the most potent analogues in this series, (*S*)-38 and (*S*)-42 (entries 2a and 6a, respectively), were found to be more potent than the corresponding racemic compounds.

2.8. Mechanism of Action of the CAI-1 Ester Analogues. We previously described a competitive antagonist (Ph-CAI-1) of the CAI-1 QS receptor CqsS.¹³ To confirm that the CAI-1 ester agonists exert their action by binding in the CAI-1 binding pocket in CqsS, we examined the effect of varying concentrations of Ph-CAI-1 on the activity of the potent analogues (*S*)-C8-ester-CAI-1 (7), 5-Ph-ester-CAI-1 (38), 4-Cy-ester-CAI-1 (40), and 1-(*p*-*n*-butyl-Ph)-ester-CAI-1 (42). All of the ester agonists examined displayed diminished potency in the presence of increasing concentrations of the competitive antagonist Ph-CAI-1 (see Supporting Information).

In an effort to elucidate the specific binding interactions that are maintained by the CAI-1 ester agonists within the CqsS

Table 5. Aryl- and Cyclohexyl-Substituted CAI-1 Ester Analogues

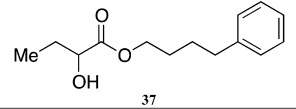
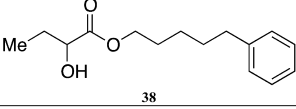
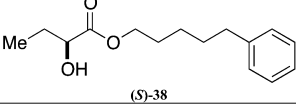
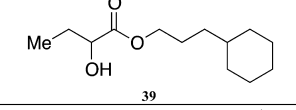
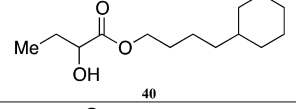
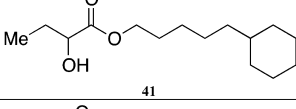
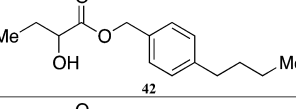
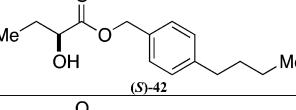
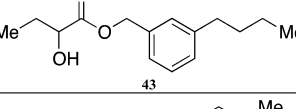
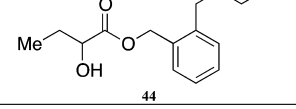
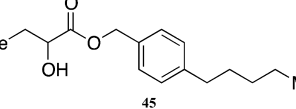
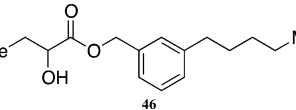
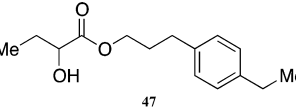
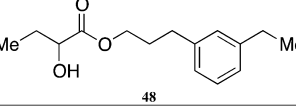
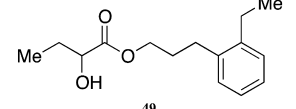
Entry	Compound	EC ₅₀ (nM) ^a	% Response ^b
1	 37	1,100±270	59±22
2	 38	231±15	93±6
2a	 (S)-38	151±20	92±13
3	 39	310±51	82±10
4	 40	84±6	97±6
5	 41	190±27	95±9
6	 42	190±19	100±6
6a	 (S)-42	117±12	94±11
7	 43	3,700±580	83±13
8	 44	>50,000	11 ^c
9	 45	680±84	85±8
10	 46	1,600±210	79±10
11	 47	190±17	98±6
12	 48	9,400±3,600	60±53
13	 49	>50,000	28 ^c

Table 5. continued

^aValues determined using a light-based CqsS agonist bioassay (see Supporting Information). All EC₅₀ values are the mean of triplicate analyses with the range defining the 95% confidence interval. ^bPercent maximal bioluminescence with respect to CAI-1, which is set at 100%. The range defines the 95% confidence interval. ^cThe maximal % response at the maximum concentration tested (50 000 nM).

binding pocket, we examined the activity of a series of agonists toward mutant CqsS receptors (Table 6). We had reported that variation in the chain length of the CAI-1 acyl tail plays a significant role in the ligand activity and that the CqsS mutant C170Y displays a preference for ligands bearing shorter acyl tails whereas the mutant C170A has a modest preference for molecules bearing longer acyl tails.¹³

The wild type CqsS receptor shows a preference for 4-Cy-ester-CAI-1 (40) with both the 5-Cy-ester-CAI-1 analogue (41) and the 3-Cy-ester-CAI-1 molecule (39) being less active (EC₅₀ higher by 2.2- to 3.7-fold, respectively). When these analogues are tested in the CqsS C170Y mutant, the higher activity shifts to the shorter 3-Cy-ester-CAI-1 analogue (39); the 4-Cy-ester-CAI-1, 40, and 5-Cy-ester-CAI-1, 41, showed EC₅₀ values 2.3-fold and 27-fold higher, respectively, compared to 39. Additionally, while the 3-Cy-ester-CAI-1, 39, was capable of inducing nearly the maximal QS response (93%), here defined with reference to C8-CAI-1 as 100% (EC₅₀ = 260 nM), the longer chain analogues 40 and 41 acted as partial agonists of this mutant receptor, inducing 51% and 66% of the maximal QS response, respectively.

While the variation in ligand preference in the C170A mutant receptor is subtle, we find that, consistent with our expectations, the longer chain 5-Cy-ester-CAI-1 analogue (41) is, among this series of ligands, uniquely capable of inducing the maximal QS response (101% maximal induction), here given with reference to CAI-1 (EC₅₀ = 72 nM), while the shorter chain analogues 39 and 41 act as partial agonists, inducing 73% and 77% of the maximal response, respectively.

In contrast, the CqsS C170A mutant receptor displayed a significantly altered response to 4-Ph-ester-CAI-1 37 and 5-Ph-ester-CAI-1 38 when compared to the wild-type response to these molecules. While both CqsS receptors prefer the longer chain, 5-Ph-ester-CAI-1 analogue (wild type CqsS EC₅₀ = 231 nM, 93% response; C170A CqsS EC₅₀ = 180 nM, 83% response), the response to the shorter 4-Ph-ester-CAI-1 analogue (37) varies significantly. Whereas 37 is a partial agonist of the wild type CqsS receptor, achieving 59% maximal response with an EC₅₀ of 1100 nM, its activity is severely diminished in the C170A mutant CqsS receptor (EC₅₀ > 50 000 nM, 16% maximal response at 50 000 nM).

Taken together, these observations provide further support for the importance of the C170 amino acid of CqsS in ligand recognition. Additionally, the CAI-1 ester analogues display a pattern of varying activity toward the CqsS C170Y and C170A mutant receptors that supports the hypothesis that these analogues bind in the CAI-1 binding pocket and elicit the QS response in a manner similar to that of the native CAI-1 molecule.

2.9. Pharmacophore Modeling. In support of the development of an antivirulence agent against *V. cholerae* that targets the CqsS QS receptor, we generated a pharmacophore model using the activity patterns observed with the CAI-1 ester analogues.^{18–20}

Table 6. Activity of CAI-1 Ester Analogues in Mutant CqsS Receptors

compd	wild-type CqsS		CqsS C170A		CqsS C170Y	
	EC ₅₀ (nM) ^a	% response ^b	EC ₅₀ (nM) ^a	% response ^b	EC ₅₀ (nM) ^a	% response ^b
(S)-CAI-1, 1	62 ± 3	100 ± 4	72 ± 21	100 ± 44	>50000	20 ^c
C8-CAI-1 ¹³	9400 ± 1600	83 ± 46	2100 ± 940	61 ± 70	260 ± 34	100 ± 8
C8-ester, 9	180 ± 170	108 ± 4	110 ± 22	99 ± 34	>50000	66 ^c
4-Ph-ester, 37	1100 ± 270	59 ± 22	>50000	16 ^c	>50000	22 ^c
5-Ph-ester, 38	231 ± 15	93 ± 6	180 ± 33	83 ± 29	>50000	19 ^c
3-Cy-ester, 39	310 ± 51	82 ± 10	790 ± 220	73 ± 28	420 ± 96	93 ± 14
4-Cy-ester, 40	84 ± 6	97 ± 6	360 ± 84	77 ± 32	960 ± 320	51 ± 48
5-Cy-ester, 41	190 ± 27	95 ± 9	1000 ± 180	101 ± 53	11000 ± 9800	66 ± 57

^aValues determined using standard light-based agonist bioassay with the designated CqsS mutant strain (see Supporting Information). All EC₅₀ values are the mean of triplicate analyses with the range defining the 95% confidence interval. ^bPercent maximal bioluminescence with respect to CAI-1, which is set at 100%. The range defines the 95% confidence interval. ^cThe maximal % response at the maximum concentration tested (50 000 nM).

The molecules used to generate the pharmacophore model display EC₅₀ < 250 nM and induced >92% of maximal response, including CAI-1 (**1**) and the CAI-1 ester analogues **9**, **26**, **38**, **40**, **41**, **42**, and **47** (Figure 5). Each of the molecules in

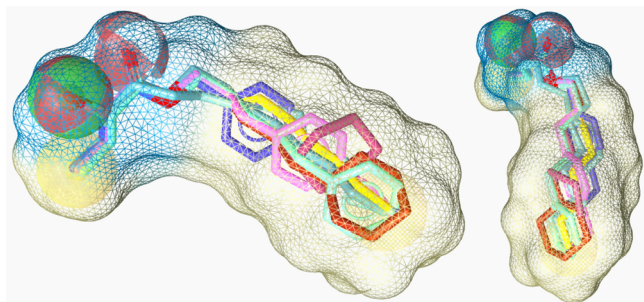


Figure 5. Pharmacophore model generated from CAI-1 (**1**, light blue) and the CAI-1 ester analogues **9** (blue-gray), **26** (yellow), **38** (light green), **40** (purple), **41** (orange), **42** (blue), and **47** (pink).

this series has a large number of energetically favorable conformations, making the identification of an optimal binding conformation difficult for any individual compound in this series. When assembled in sum, however, we find that the structures of the active compounds converge to provide a unified model of the CqsS binding pocket. Indeed, among the best-fit pharmacophore models generated, only subtle variation was observed in the overall molecular topology of the ligand binding surface. Together with our chemical genetic analyses of CqsS, this model provides reasonable detail of the ligand–receptor binding interaction within the transmembrane region of CqsS in the absence of more detailed structural information about this receptor (e.g., X-ray crystallographic analysis).

Consistent with our SAR, this model suggests the presence of a fairly large hydrophobic binding pocket into which the acyl tail of the CAI-1 molecule projects. From the benzene and cyclohexane analogues, it is clear that the binding pocket tolerates significant additional steric bulk along the entire length of the hydrophobic tail. This feature results in a combined hydrophobic surface described by the model that is significantly larger than the van der Waals surface of the saturated acyl tail of CAI-1.

To test the validity of this model, we examined the fit of ligands that displayed diminished activity, predicting that these analogues would not fit well in the optimized pharmacophore model. We selected a series of compounds that varied in their

ability to agonize CqsS in order to test the prediction that compounds displaying moderate activity would be subtly perturbed from this model whereas compounds that displayed low activity would possess greater deviations from the ideal molecular topology described by this model. The less potent CAI-1 ester analogues deviate from the model (Figure 6); the

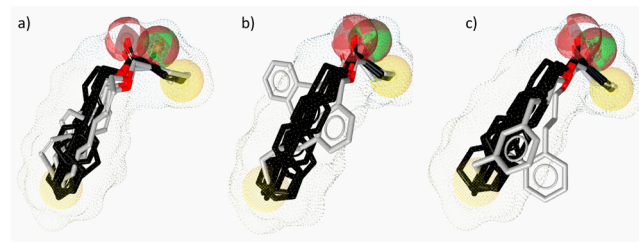


Figure 6. Images highlighting the deviation of less active CAI-1 ester analogues (shown in gray) from the pharmacophore model. Active analogues used to generate the pharmacophore model are shown in black with the combined VDW surface highlighted with points. (a) CAI-1 ester analogues containing a (Z)-olefin in the 2, 3, 4, or 5 position (**27**, **30**, **33**, and **35**). (b) Ortho- and meta-butyl substituted aryl CAI-1 ester analogues **43** and **44**. (c) Ortho- and meta-ethyl substituted aryl CAI-1 ester analogues **48** and **49**.

extent of deviation appears to generally correlate with the biological activity. For example, 2-(Z)-, 3-(Z)-, 4-(Z)-, and 5-(Z)-C8-ester-CAI-1 (**27**, **30**, **33**, and **35**) that fully activate the QS response but are >3-fold less active than the saturated analogue **9** all deviate clearly from the pharmacophore model (Figure 6a). However, the extent to which these analogues deviate from the model is less pronounced than the deviation of the still less potent 1,3-substituted phenyl analogues **43** and **48** (<83% maximal response, EC₅₀ being >21-fold higher than that for **9**). The 1,2-substituted phenyl analogues **44** and **49** (<28% maximal response, EC₅₀ being >278-fold higher than that for **9**) display even more pronounced deviations from the model (Figure 6b and Figure 6c). While the pharmacophore model correlates with the biological activity of the majority of the analogues, there are two analogues for which the model is not consistent. The 3-(E)-, and 5-(E)-C8-ester-CAI-1 analogues **29** and **34** appear to fully satisfy the model, and yet these analogues are only modest agonists, fully activating the QS response but with EC₅₀ values being >4-fold higher than that of the saturated analogue **9** (see Supporting Information). Notwithstanding these exceptions, this model approximates the molecular topology of the binding pocket for the fatty acid

tail portion of the CAI-1 ligands and effectively correlates with the biological activity for most of the analogues examined; it represents a finding that should be of general interest for further studies of this class of membrane associated receptors.

3. CONCLUSION

Synthetic molecules that act as agonists of QS in *V. cholerae* represent useful tools to enhance our understanding of QS and the mechanisms for controlling virulence in this globally relevant human pathogen. A series of rationally designed CAI-1 analogues was prepared to examine the preference of the receptor to structural changes within the fatty acid derived tail portion of the CAI-1 signaling molecule. The construction of this compound library was facilitated by the discovery that the CAI-1 α -hydroxy ester analogues display comparable activity and SAR to the parent CAI-1 α -hydroxy ketones. We note that the conformational and electronic differences between the ester and ketone functionality make this an interesting example of an ester serving as a suitable bioisostere for a ketone.^{21,22} Further complicating the use of esters as biological probes, esters are subject to the activity of ubiquitous esterases, a feature that has been capitalized on in the design of prodrugs.^{23,24} We find that the alcohol tails for several of the most potent analogues, the products of esterase cleavage, show no QS activity up to 50 000 nM. Similarly, the conserved esterase cleavage product, 2-hydroxybutyric acid, displays no activity at concentrations up to 50 000 nM. Accordingly, we believe that the esters described in this study are not undergoing cleavage prior to activation of the QS response. Rather, the esters themselves serve as activators of QS by interacting with the membrane-associated receptor CqsS in a manner similar to the native signal, CAI-1.

The membrane-bound QS receptor in *V. cholerae* tolerates several structural changes deviating from the fully saturated linear alkyl tail contained in the native signaling molecule, including both conformational restrictions in the acyl tail and the incorporation of branched functionality in the form of phenyl and cyclohexyl rings. Examination of SAR for this series of analogues was used to generate a model for the structural constraints on the ligand allowable by the CqsS QS receptor. This is significant, as the receptor is membrane-associated which complicates the acquisition of detailed structural information, for example, through X-ray crystallographic studies. These results, together with chemical genetics, provide crucial information about the molecular topology and localization of the ligand binding pocket of CqsS that will be broadly useful to diverse studies of this important bacterial pathogen.

4. EXPERIMENTAL METHODS

General Experimental. Unless otherwise noted, all reactions were performed in flame-dried glassware under an atmosphere of nitrogen or argon using dried reagents and solvents. All chemicals were purchased from commercial vendors and used without further purification, and anhydrous solvents were purchased from commercial vendors.

Flash chromatography was performed using standard grade silica gel 60 230–400 mesh from SORBENT Technologies. Analytical thin-layer chromatography was carried out using silica G TLC plates, 200 μ m with UV₂₅₄ fluorescent indicator (SORBENT Technologies), and visualization was performed by staining and/or by absorbance of UV light.

NMR spectra were recorded using a Bruker Avance II (500 MHz for ¹H, 125 MHz for ¹³C) spectrometer fitted with either a ¹H-optimized TCI (H/C/N) cryoprobe or a ¹³C-optimized dual C/H cryoprobe. Chemical shifts are reported in parts per million (ppm) and

were calibrated according to residual protonated solvent. High-resolution mass spectral analysis was performed using an Agilent 1200 series electrospray ionization, time-of-flight (ESI-TOF) mass spectrometer in the positive ESI mode. Analytical high-performance liquid chromatography was performed by Lotus Separations, LLC, using a Rainin HPLC with SD-1 pumps and a Dynamax UV-1 detector. Supercritical fluid chromatography was performed by Lotus Separations, LLC, using a Berger Multigram II SFC with Rainin SD-1 pumps and a Knauer K-2501 spectrophotometer. All final compounds were determined to be of >95% purity by analysis of their characterization data.

Typical Procedure for the Synthesis of CAI-1 Analogues 9, 10, and 22–25. Method A. To a solution of the α -hydroxy acid (1.0 equiv) in DMF (1.5M) at room temperature were added imidazole (3.0 equiv) and *tert*-butyldimethylsilyl chloride (3.0 equiv). The mixture was stirred at room temperature overnight. The reaction was quenched with hydrochloric acid (1 N), and extraction was with ethyl acetate (EtOAc). The sample was washed with H₂O and brine, dried over Na₂SO₄, and concentrated in vacuo. The residue was treated with SOCl₂ (6.6 equiv) and heated to reflux overnight. Excess SOCl₂ was removed in vacuo, and the product was used for the next reaction step without further purification. To a solution of primary alcohol (1.0 equiv) and DMAP (1.1 equiv) in THF (0.13M) at room temperature was added the acid chloride obtained in the previous step (1.1 equiv), dropwise. The mixture was allowed to stir overnight at room temperature and was concentrated in vacuo to form a slurry which was purified by silica gel chromatography. The purified TBS-protected intermediate in THF (1M) was treated with TBAF (3 equiv), and the mixture was allowed to stir overnight before direct concentration and purification by silica gel chromatography.

Typical Procedure for the Synthesis of CAI-1 Ester Analogues 7, 8, 17–21, and 26–49. Method B. Molecular sieves (5 Å powdered, 0.5 g/mmol of ester) and the carbene catalyst (0.1 equiv) were added to a screw-top vial equipped with a stir bar. The vial was evacuated and purged with N₂ three times before being placed under nitrogen. To the vial was added PhMe (0.5M), ethyl 2-hydroxybutyrate (1 equiv), and the primary alcohol (2 equiv). The reaction mixture was stirred overnight at room temperature, was directly concentrated, and the residue was purified by silica gel chromatography.

Octyl 2-Hydroxybutanoate, 9. 9 was prepared according to method A to provide octyl 2-hydroxybutanoate (20 mg, 24% yield, four steps). 9 was also prepared according to method B, using 1-octanol to provide octyl 2-hydroxybutanoate (86 mg, 40% yield). ¹H NMR (500 MHz, CDCl₃) δ 4.22–4.09 (m, 3H), 2.74 (d, *J* = 5.5 Hz, 1H), 1.87–1.77 (m, 1H), 1.72–1.59 (m, 3H), 1.37–1.18 (m, 10H), 0.94 (t, *J* = 7.4 Hz, 3H), 0.86 (t, *J* = 6.9 Hz, 3H). ¹³C NMR (126 MHz, CDCl₃) δ 175.6, 77.5, 77.2, 77.0, 66.0, 32.0, 29.4, 29.3, 28.7, 27.7, 26.0, 22.8. HRMS (ESI-TOF) calculated for C₁₂H₂₅O₃ [M + H]⁺, 217.1804; observed, 217.1794.

(S)-2-Hydroxy-N-octylbutanamide, 10. 10 was prepared according to method A, providing (S)-2-hydroxy-N-octylbutanamide (44 mg, 53% yield, four steps). ¹H NMR (500 MHz, CDCl₃) δ 6.69–6.57 (brs, 1H), 4.02 (dd, *J* = 3.8, 7.0 Hz, 1H), 3.38–3.13 (m, 3H), 1.89–1.76 (m, 1H), 1.71–1.58 (m, 1H), 1.54–1.43 (m, 2H), 1.35–1.14 (m, 10H), 0.95 (t, *J* = 7.4 Hz, 3H), 0.83 (t, *J* = 6.7 Hz, 3H). ¹³C NMR (125 MHz, CDCl₃) δ 173.8, 73.0, 39.1, 31.8, 29.6, 29.3, 29.2, 27.9, 26.9, 22.7, 14.1, 9.1. HRMS (ESI-TOF) calculated for C₁₂H₂₆NO₂ [M + H]⁺, 216.1958; found 216.1974.

2-(Pentyloxy)ethyl 2-Hydroxybutanoate, 22. 22 was prepared according to method A, giving 2-(pentyloxy)ethyl 2-hydroxybutanoate (77.8 mg, 22% yield, four steps). ¹H NMR (500 MHz, CDCl₃) δ 4.37–4.26 (m, 2H), 4.18 (dd, *J* = 5.1, 10.5 Hz, 1H), 3.63 (t, *J* = 4.7 Hz, 2H), 3.43 (t, *J* = 6.7 Hz, 2H), 2.73 (d, *J* = 5.4 Hz, 1H), 1.88–1.79 (m, 1H), 1.73–1.64 (m, 1H), 1.61–1.52 (m, 2H), 1.32–1.26 (m, 4H), 0.95 (t, *J* = 7.4 Hz, 3H), 0.87 (t, *J* = 6.8 Hz, 3H). ¹³C NMR (125 MHz, CDCl₃) δ 175.3, 71.5, 71.4, 68.3, 64.6, 29.3, 28.2, 27.5, 22.5, 14.1, 8.9. HRMS (ESI-TOF) calculated for C₁₁H₂₃O₄ [M + H]⁺, 219.1591; found 219.1592.

2-Hydroxy-2-(2-ethoxyethoxy)ethylbutanoate, 23. 23 was prepared according to method A, giving 2-hydroxy-2-(2-ethoxyethoxy)ethylbutanoate (0.349 g, 60% yield, four steps). ^1H NMR (500 MHz, CDCl_3) δ 4.39–4.26 (m, 2H), 4.17 (dd, $J = 5.7, 10.9$ Hz, 1H), 3.72 (t, $J = 4.7$ Hz, 2H), 3.65–3.61 (m, 2H), 3.59–3.56 (m, 2H), 3.50 (dd, $J = 7.0, 14.0$ Hz, 2H), 2.74 (d, $J = 5.7$ Hz, 1H), 1.88–1.79 (m, 1H), 1.74–1.63 (m, 1H), 1.20 (t, $J = 7.0$ Hz, 3H), 0.95 (t, $J = 7.4$ Hz, 3H). ^{13}C NMR (125 MHz, CDCl_3) δ 175.4, 71.4, 70.7, 69.8, 68.9, 66.8, 64.5, 27.5, 15.2, 8.9. HRMS (ESI-TOF) calculated for $\text{C}_{10}\text{H}_{21}\text{O}_5$ $[\text{M} + \text{H}]^+$, 221.1384; found 221.1389.

2-(Hexyloxy)ethyl 2-Hydroxybutanoate, 24. 24 was prepared according to method A, giving 2-(hexyloxy)ethyl 2-hydroxybutanoate (0.163g, 19% yield, four steps). ^1H NMR (500 MHz, CDCl_3) δ 4.34–4.21 (m, 2H), 4.13 (dd, 1H, $J = 4.2, 8.8$ Hz), 3.58 (t, 2H, $J = 4.7$ Hz), 3.38 (t, 2H, $J = 6.7$ Hz), 2.67 (d, 1H, $J = 5.8$ Hz), 1.86–1.74 (m, 1H), 1.69–1.57 (m, 1H), 1.51–1.46 (m, 2H), 1.31–1.16 (m, 6H), 0.92–0.88 (m, 3H), 0.82 (t, 3H, $J = 6.9$ Hz). ^{13}C NMR (125 MHz, CDCl_3) δ 175.4, 71.5, 71.4, 68.3, 64.7, 31.7, 29.6, 27.5, 25.8, 22.7, 14.1, 8.9. HRMS (ESI-TOF) calculated for $\text{C}_{12}\text{H}_{25}\text{O}_4$ $[\text{M} + \text{H}]^+$, 233.1747; found 233.1752.

2-Hydroxy-2-(2-(2-methoxyethoxy)ethoxy)ethylbutanoate, 25. 25 was prepared according to method A, giving 2-hydroxy-2-(2-(2-methoxyethoxy)ethoxy)ethylbutanoate (412 mg, 54% yield, four steps). ^1H NMR (500 MHz, CDCl_3) δ 4.37–4.29 (m, 2H), 4.19–4.15 (m, 1H), 3.70 (t, $J = 4.7$ Hz, 2H), 3.66–3.60 (m, 4H), 3.55–3.51 (m, 2H), 3.36 (s, 2H), 2.90 (d, $J = 5.8$ Hz, 1H), 1.88–1.78 (m, 1H), 1.73–1.64 (m, 1H), 1.62 (s, 3H), 0.98–0.92 (t, $J = 7.4$ Hz, 3H). ^{13}C NMR (125 MHz, CDCl_3) δ 175.2, 71.9, 71.5, 70.6, 70.6, 70.6, 68.9, 64.5, 59.1, 27.5, 9.0. HRMS (ESI-TOF) calculated for $\text{C}_{11}\text{H}_{22}\text{O}_6\text{Na}$ $[\text{M} + \text{Na}]^+$, 273.1309; found 273.1316.

(S)-2-Aminoocetylbutanoate Hydrochloride, 12. To L-amino-butyric acid (500 mg, 4.83 mmol) were added octanol (40.3 mL) and 2 M HCl/ether (7.0 mL). The mixture was heated to reflux (150 °C) for 24 h and was concentrated in vacuo. When the mixture was cooled, a solid was formed which was dissolved in ethyl acetate with warming. The solution was left overnight to form crystals which were subsequently filtered and air-dried, giving (S)-2-aminoocetylbutanoate hydrochloride (0.611g, 50% yield). ^1H NMR (500 MHz, CDCl_3) δ 8.97–8.83 (brs, 2H), 4.31–4.16 (m, 2H), 4.06 (t, $J = 5.8$ Hz, 1H), 2.22–2.06 (m, 2H), 1.76–1.64 (m, 2H), 1.42–1.23 (m, 10H), 1.15 (t, $J = 7.5$ Hz, 3H), 0.91 (t, $J = 6.9$ Hz, 3H). ^{13}C NMR (125 MHz, CDCl_3) δ 169.2, 66.8, 54.5, 32.0, 29.4, 29.3, 28.6, 25.9, 24.1, 22.8, 14.3, 9.7. HRMS (ESI-TOF) calculated for $\text{C}_{12}\text{H}_{26}\text{NO}_2$ $[\text{M} + \text{H}]^+$, 216.1958; found 216.1959.

(R)-2-Aminoocetylbutanoate Hydrochloride, 13. 13 was prepared following the procedure for the synthesis of octyl 2-hydroxybutanoate (12) from D-aminobutyric acid. ^1H NMR (500 MHz, CDCl_3) δ 8.96–8.84 (brs, 2H), 4.30–4.14 (m, 2H), 4.07 (t, $J = 5.8, 1\text{H}$), 2.20–2.08 (m, 2H), 1.75–1.64 (m, 2H), 1.39–1.24 (m, 10H), 1.14 (t, $J = 7.5$ Hz, 3H), 0.91 (t, $J = 6.9$ Hz, 3H). ^{13}C NMR (125 MHz, CDCl_3) δ 169.1, 66.7, 54.3, 31.8, 29.2, 29.2, 28.4, 25.8, 24.0, 22.7, 14.2, 9.5. HRMS (ESI-TOF) calculated for $\text{C}_{12}\text{H}_{26}\text{NO}_2$ $[\text{M} + \text{H}]^+$, 216.1958; found 216.1965.

(S)-Octyl 2-Hydroxybutanoate, 7. 7 was prepared according to method B, using (S)-methyl 2-hydroxybutanoate²⁵ and octanol to provide (S)-octyl 2-hydroxybutanoate as a clear colorless oil (55 mg, 40%). ^1H NMR (500 MHz, CDCl_3) δ 4.17–4.11 (m, 3H), 2.74 (d, $J = 5.5$ Hz, 1H), 1.88–1.77 (m, 1H), 1.72–1.59 (m, 3H), 1.38–1.19 (m, 10H), 0.94 (t, $J = 7.4$ Hz, 3H), 0.86 (t, $J = 6.9$ Hz, 3H). ^{13}C NMR (126 MHz, CDCl_3) δ 175.6, 77.5, 77.2, 77.0, 66.0, 32.0, 29.4, 29.3, 28.7, 27.7, 26.0, 22.8. HRMS (ESI-TOF) calculated for $\text{C}_{12}\text{H}_{25}\text{O}_3$ $[\text{M} + \text{H}]^+$, 217.1804; observed, 217.1794.

(R)-Octyl 2-hydroxybutanoate, 8. 8 was prepared according to method B from (R)-methyl 2-hydroxybutanoate and octanol to provide (R)-octyl 2-hydroxybutanoate as a clear colorless oil. ^1H NMR (500 MHz, CDCl_3) δ 4.17–4.11 (m, 3H), 2.73 (d, $J = 5.7$ Hz, 1H), 1.87–1.77 (m, 1H), 1.72–1.54 (m, 3H), 1.38–1.19 (m, 10H), 0.94 (t, $J = 7.4$ Hz, 3H), 0.86 (t, $J = 7.0$ Hz, 3H). ^{13}C NMR (126 MHz, CDCl_3) δ 175.6, 77.5, 77.2, 77.0, 66.0, 32.0, 29.4, 29.3, 28.7, 27.7, 26.0,

22.8. HRMS (ESI-TOF) calculated for $\text{C}_{12}\text{H}_{25}\text{O}_3$ $[\text{M} + \text{H}]^+$, 217.1804; observed, 217.1793.

Butyl 2-Hydroxybutanoate, 17. 17 was prepared according to method B, using 1-butanol to provide butyl 2-hydroxybutanoate (29 mg, 20% yield). ^1H NMR (500 MHz, CDCl_3) δ 4.22–4.04 (m, 3H), 2.88 (bs, 1H), 1.86–1.74 (m, 1H), 1.68–1.56 (m, 3H), 1.38–1.30 (m, 2H), 0.92 (t, $J = 7.5$ Hz, 3H), 0.89 (t, $J = 7.4$ Hz, 3H). ^{13}C NMR (126 MHz, CDCl_3) δ 175.5, 71.5, 65.6, 30.7, 27.7, 19.2, 13.8, 9.1. HRMS (ESI-TOF) calculated for $\text{C}_8\text{H}_{17}\text{O}_3\text{Na}$ $[\text{M} + \text{Na}]^+$, 183.0997; observed, 183.0992.

Hexyl 2-Hydroxybutanoate, 18. 18 was prepared according to method B, using 1-hexanol (250 μL , 2.0 mmol) to provide hexyl 2-hydroxybutanoate (105 mg, 56% yield). ^1H NMR (500 MHz, CDCl_3) δ 4.22–4.10 (m, 3H), 2.75 (d, $J = 5.7$ Hz, 1H), 1.87–1.77 (m, 1H), 1.70–1.59 (m, 3H), 1.38–1.22 (m, 6H), 0.94 (t, $J = 7.4$ Hz, 3H), 0.87 (t, $J = 6.8$ Hz, 3H). ^{13}C NMR (125 MHz, CDCl_3) δ 175.6, 71.5, 66.0, 31.5, 28.7, 27.7, 25.7, 22.7, 14.2, 9.1. HRMS (ESI-TOF) calculated for $\text{C}_{10}\text{H}_{21}\text{O}_3$ $[\text{M} + \text{H}]^+$, 189.1491; observed, 189.1500.

Heptyl 2-Hydroxybutanoate, 19. 19 was prepared according to method B, using 1-heptanol to provide heptyl 2-hydroxybutanoate (60 mg, 30% yield). ^1H NMR (500 MHz, CDCl_3) δ 4.21–4.10 (m, 3H), 2.75 (d, $J = 5.7$ Hz, 1H), 1.87–1.76 (m, 1H), 1.70–1.59 (m, 3H), 1.37–1.20 (m, 8H), 0.94 (t, $J = 7.4$ Hz, 3H), 0.86 (t, $J = 7.0$ Hz, 3H). ^{13}C NMR (125 MHz, CDCl_3) δ 175.6, 71.5, 66.0, 31.9, 29.1, 28.7, 27.7, 26.0, 22.8, 14.3, 9.1. HRMS (ESI-TOF) calculated for $\text{C}_{11}\text{H}_{23}\text{O}_3$ $[\text{M} + \text{H}]^+$, 203.1647; observed, 203.1650.

Nonyl 2-Hydroxybutanoate, 20. 20 was prepared according to method B, using 1-nonanol to provide nonyl 2-hydroxybutanoate (143 mg, 62% yield). ^1H NMR (500 MHz, CDCl_3) δ 4.23–4.09 (m, 3H), 2.77 (d, $J = 5.2$ Hz, 1H), 1.87–1.76 (m, 1H), 1.70–1.56 (m, 3H), 1.38–1.16 (m, 12H), 0.94 (t, $J = 7.4$ Hz, 3H), 0.85 (t, $J = 6.9$ Hz, 3H). ^{13}C NMR (125 MHz, CDCl_3) δ 175.6, 71.5, 66.0, 32.0, 29.6, 29.4, 29.4, 28.7, 27.7, 26.0, 22.9, 14.3, 9.1. HRMS (ESI-TOF) calculated for $\text{C}_{13}\text{H}_{27}\text{O}_3$ $[\text{M} + \text{H}]^+$, 231.1960; observed, 231.1961.

Decyl 2-Hydroxybutanoate, 21. 21 was prepared according to method B, using 1-decanol to provide decyl 2-hydroxybutanoate (158 mg, 65% yield). ^1H NMR (500 MHz, CDCl_3) δ 4.22–4.09 (m, 3H), 2.75 (d, $J = 5.5$ Hz, 1H), 1.87–1.76 (m, 1H), 1.70–1.59 (m, 3H), 1.37–1.17 (m, 14H), 0.94 (t, $J = 7.4$ Hz, 3H), 0.85 (t, $J = 6.9$ Hz, 3H). ^{13}C NMR (126 MHz, CDCl_3) δ 175.4, 71.3, 65.9, 31.9, 29.5, 29.5, 29.3, 29.2, 28.6, 27.5, 25.8, 22.7, 14.2, 8.9. HRMS (ESI-TOF) calculated for $\text{C}_{14}\text{H}_{29}\text{O}_3$ $[\text{M} + \text{H}]^+$, 245.2117; observed, 245.2122.

(E)-Oct-2-en-1-yl 2-Hydroxybutanoate, 26. 26 was prepared according to method B, using (E)-2-octen-1-ol to provide (E)-oct-2-en-1-yl 2-hydroxybutanoate (134 mg, 63% yield). ^1H NMR (500 MHz, CDCl_3) δ 5.83–5.74 (m, 1H), 5.59–5.49 (m, 1H), 4.65–4.55 (m, 2H), 4.14 (dd, $J = 6.2, 4.7$ Hz, 1H), 2.73 (bs, 1H), 2.03 (q, $J = 7.1$ Hz, 2H), 1.87–1.77 (m, 1H), 1.71–1.61 (m, 1H), 1.40–1.31 (m, 2H), 1.31–1.21 (m, 4H), 0.94 (t, $J = 7.4$ Hz, 3H), 0.86 (t, $J = 6.9$ Hz, 3H). ^{13}C NMR (126 MHz, CDCl_3) δ 175.3, 138.0, 123.2, 71.6, 66.6, 32.4, 31.5, 28.7, 27.7, 22.7, 14.3, 9.1. HRMS (ESI-TOF) calculated for $\text{C}_{12}\text{H}_{22}\text{O}_3\text{Na}$ $[\text{M} + \text{Na}]^+$, 237.1466; observed, 237.1470.

(Z)-Oct-2-en-1-yl 2-Hydroxybutanoate, 27. 27 was prepared according to method B, using (Z)-2-octen-1-ol to provide (Z)-oct-2-en-1-yl 2-hydroxybutanoate (180 mg, 84% yield). ^1H NMR (500 MHz, CDCl_3) δ 5.71–5.62 (m, 1H), 5.55–5.46 (m, 1H), 4.77–4.65 (m, 2H), 4.14 (s, 1H), 2.74 (s, 1H), 2.08 (q, $J = 7.3$ Hz, 2H), 1.87–1.76 (m, 1H), 1.73–1.60 (m, 1H), 1.40–1.21 (m, 6H), 0.93 (t, $J = 7.4$ Hz, 3H), 0.86 (t, $J = 6.9$ Hz, 3H). ^{13}C NMR (126 MHz, CDCl_3) δ 175.4, 136.7, 122.6, 71.6, 61.6, 31.6, 29.2, 27.7, 27.7, 22.7, 14.3, 9.1. HRMS (ESI-TOF) calculated for $\text{C}_{12}\text{H}_{22}\text{O}_3\text{Na}$ $[\text{M} + \text{Na}]^+$, 237.1466; observed, 237.1471.

Oct-2-yn-1-yl 2-Hydroxybutanoate, 28. 28 was prepared according to method B, using 2-octyn-1-ol to provide oct-2-yn-1-yl 2-hydroxybutanoate (102 mg, 48% yield). ^1H NMR (500 MHz, CDCl_3) δ 4.80–4.70 (m, 2H), 4.19 (dd, $J = 6.3, 4.4$ Hz, 1H), 2.67 (s, 1H), 2.22–2.15 (m, 2H), 1.89–1.79 (m, 1H), 1.76–1.65 (m, 1H), 1.53–1.44 (m, 2H), 1.37–1.24 (m, 4H), 0.95 (t, $J = 7.4$ Hz, 3H), 0.87 (t, $J = 7.0$ Hz, 3H). ^{13}C NMR (126 MHz, CDCl_3) δ 174.9, 88.7, 73.4,

71.5, 54.1, 31.2, 28.2, 27.6, 22.4, 18.9, 14.2, 9.0. HRMS (ESI-TOF) calculated for $C_{12}H_{20}O_3Na$ $[M + Na]^+$, 235.1310; observed, 235.1310.

(E)-Oct-3-en-1-yl 2-Hydroxybutanoate, 29. 29 was prepared according to method B, using (E)-3-octen-1-ol to provide (E)-oct-3-en-1-yl 2-hydroxybutanoate (88 mg, 98% yield). 1H NMR (500 MHz, $CDCl_3$) δ 5.54–5.44 (m, 1H), 5.36–5.26 (m, 1H), 4.23–4.07 (m, 3H), 2.79 (s, 1H), 2.32 (q, J = 6.7 Hz, 2H), 2.00–1.90 (m, 2H), 1.84–1.74 (m, 1H), 1.70–1.58 (m, 1H), 1.34–1.19 (m, 4H), 0.93 (t, J = 7.4 Hz, 3H), 0.85 (t, J = 7.0 Hz, 3H). ^{13}C NMR (126 MHz, $CDCl_3$) δ 175.5, 134.2, 124.7, 71.5, 65.4, 32.5, 32.1, 31.7, 27.7, 22.3, 14.1, 9.1. HRMS (ESI-TOF) calculated for $C_{12}H_{22}O_3Na$ $[M + Na]^+$, 237.1466; observed, 237.1475.

(Z)-Oct-3-en-1-yl 2-Hydroxybutanoate, 30. 30 was prepared according to method B, using (Z)-3-octen-1-ol to provide (Z)-oct-3-en-1-yl 2-hydroxybutanoate (60 mg, 30% yield). 1H NMR (500 MHz, $CDCl_3$) δ 5.55–5.43 (m, 1H), 5.34–5.23 (m, 1H), 4.21–4.08 (m, 3H), 2.79 (d, J = 3.4 Hz, 1H), 2.38 (q, J = 7.0 Hz, 2H), 2.08–1.95 (m, 1H), 1.84–1.74 (m, 1H), 1.69–1.59 (m, 1H), 1.34–1.24 (m, 4H), 0.93 (t, J = 7.5 Hz, 3H), 0.87 (t, J = 7.0 Hz, 3H). ^{13}C NMR (126 MHz, $CDCl_3$) δ 175.5, 133.5, 123.9, 71.6, 65.2, 31.9, 27.7, 27.2, 27.0, 22.5, 14.1, 9.1. HRMS (ESI-TOF) calculated for $C_{12}H_{22}O_3Na$ $[M + Na]^+$, 237.1466; observed, 237.1475.

Oct-3-yn-1-yl 2-Hydroxybutanoate, 31. 31 was prepared according to method B, using 3-octyn-1-ol to provide oct-3-yn-1-yl 2-hydroxybutanoate (110 mg, 52% yield). 1H NMR (500 MHz, $CDCl_3$) δ 4.29–4.13 (m, 3H), 2.70 (s, 1H), 2.54–2.46 (m, 2H), 2.14–2.07 (m, 2H), 1.88–1.77 (m, 1H), 1.74–1.62 (m, 1H), 1.47–1.31 (m, 4H), 0.95 (t, J = 7.4 Hz, 3H), 0.88 (t, J = 7.2 Hz, 3H). ^{13}C NMR (126 MHz, $CDCl_3$) δ 175.3, 82.5, 75.2, 71.5, 64.1, 31.1, 27.7, 22.1, 19.5, 18.5, 13.8, 9.1. HRMS (ESI-TOF) calculated for $C_{12}H_{20}O_3Na$ $[M + Na]^+$, 235.1310; observed, 235.1313.

(E)-Oct-4-enyl 2-Hydroxybutanoate, 32. 32 was prepared according to method B, using (E)-4-octyn-1-ol to provide (E)-oct-4-enyl 2-hydroxybutanoate (69.9 mg, 75% yield). 1H NMR (500 MHz, $CDCl_3$) δ 5.46–5.29 (m, 2H), 4.22–4.09 (m, 3H), 2.75 (s, 1H), 2.04 (q, J = 7.0 Hz, 2H), 1.93 (q, J = 6.9 Hz, 2H), 1.87–1.77 (m, 1H), 1.74–1.62 (m, 3H), 1.39–1.29 (m, 2H), 0.94 (t, J = 7.4 Hz, 3H), 0.86 (t, J = 7.4 Hz, 3H). ^{13}C NMR (125 MHz, $CDCl_3$) δ 175.6, 131.9, 128.7, 71.5, 65.3, 34.8, 28.9, 28.6, 27.7, 22.8, 13.9, 9.1. HRMS (ESI-TOF) calculated for $C_{12}H_{23}O_3$ $[M + H]^+$, 215.1647; observed, 215.1644.

(Z)-Oct-4-enyl 2-Hydroxybutanoate, 33. 33 was prepared according to method B, using (Z)-4-octyn-1-ol to provide (Z)-oct-4-enyl 2-hydroxybutanoate (42.7 mg, 55% yield). 1H NMR (500 MHz, $CDCl_3$) δ 5.45–5.27 (m, 2H), 4.23–4.09 (m, 3H), 2.76 (d, J = 5.7 Hz, 1H), 2.09 (q, J = 7.3 Hz, 2H), 1.97 (q, J = 7.3 Hz, 2H), 1.88–1.77 (m, 1H), 1.76–1.62 (m, 3H), 1.39–1.28 (m, 2H), 0.95 (t, J = 7.4 Hz, 3H), 0.87 (t, J = 7.2 Hz, 3H). ^{13}C NMR (125 MHz, $CDCl_3$) δ 175.5, 131.4, 128.2, 71.5, 65.4, 29.5, 28.7, 27.7, 23.6, 23.0, 14.0, 9.1. HRMS (ESI-TOF) calculated for $C_{12}H_{23}O_3$ $[M + H]^+$, 215.1647; observed, 215.1646.

(E)-Oct-5-enyl 2-Hydroxybutanoate, 34. 34 was prepared according to method B, using (E)-5-octyn-1-ol to provide (E)-oct-5-enyl 2-hydroxybutanoate (41.3 mg, 65% yield). 1H NMR (500 MHz, $CDCl_3$) δ 5.49–5.29 (m, 2H), 4.23–4.09 (m, 3H), 2.74 (d, J = 5.7 Hz, 1H), 2.04–1.93 (m, 4H), 1.86–1.78 (m, 1H), 1.71–1.59 (m, 3H), 1.44–1.35 (m, 2H), 0.94 (t, J = 7.4 Hz, 6H). ^{13}C NMR (125 MHz, $CDCl_3$) δ 175.6, 133.0, 128.5, 71.5, 65.8, 32.2, 28.2, 27.7, 25.9, 25.8, 14.2, 9.1. HRMS (ESI-TOF) calculated for $C_{12}H_{23}O_3$ $[M + H]^+$, 215.1647; observed, 215.1642.

(Z)-Oct-5-en-1-yl 2-Hydroxybutanoate, 35. 35 was prepared according to method B, using (Z)-5-octen-1-ol to provide (Z)-oct-5-en-1-yl 2-hydroxybutanoate (116 mg, 78% yield). 1H NMR (500 MHz, $CDCl_3$) δ 5.42–5.34 (m, 1H), 5.32–5.23 (m, 1H), 4.23–4.09 (m, 3H), 2.09–1.96 (m, 4H), 1.86–1.77 (m, 1H), 1.70–1.61 (m, 3H), 1.45–1.35 (m, 2H), 0.99–0.88 (m, 6H). ^{13}C NMR (126 MHz, $CDCl_3$) δ 175.6, 132.6, 128.4, 71.5, 65.8, 28.3, 27.7, 26.7, 26.1, 20.7, 14.6, 9.1. HRMS (ESI-TOF) calculated for $C_{12}H_{22}O_3Na$ $[M + Na]^+$, 237.1466; observed, 237.1472.

(2-Pentylcyclopropyl)methyl 2-Hydroxybutanoate, 36. 36 was prepared according to method B, using (2-pentylcyclopropyl)methanol to provide (2-pentylcyclopropyl)methyl 2-hydroxybutanoate as a mixture of stereoisomers (23.7 mg, 60% yield). 1H NMR (500 MHz, $CDCl_3$) δ 4.17–4.11 (m, 1H), 4.10–3.90 (m, 2H), 2.76 (d, J = 5.6 Hz, 1H), 1.89–1.78 (m, 1H), 1.73–1.62 (m, 1H), 1.39–1.20 (m, 7H), 1.18–1.08 (m, 1H), 0.95 (t, J = 7.4 Hz, 3H), 0.86 (t, J = 6.9 Hz, 3H), 0.70–0.61 (m, 1H), 0.45–0.38 (m, 1H), 0.38–0.31 (m, 1H). ^{13}C NMR (126 MHz, $CDCl_3$) δ 175.63, 71.6, 71.5, 70.4, 70.3, 33.6, 31.8, 29.3, 29.3, 27.7, 22.9, 18.1, 18.0, 17.3, 17.3, 14.3, 10.7, 10.7, 9.1, 9.1. HRMS (ESI-TOF) calculated for $C_{13}H_{25}O_3$ $[M + H]^+$, 229.1804; observed, 229.1810.

4-Phenylbutyl 2-Hydroxybutyrate, 37. 37 was prepared according to method B, using 4-phenyl-1-butanol to provide 4-phenylbutyl 2-hydroxybutyrate (200 mg, 85% yield). 1H NMR (500 MHz, $CDCl_3$) δ 7.30–7.22 (m, 2H), 7.21–7.13 (m, 3H), 4.25–4.14 (m, 2H), 4.13 (dd, J = 6.6, 4.4 Hz, 1H), 2.70 (s, 1H), 2.67–2.57 (m, 2H), 1.87–1.76 (m, 1H), 1.73–1.61 (m, 5H), 0.94 (t, J = 7.4 Hz, 3H). ^{13}C NMR (126 MHz, $CDCl_3$) δ 175.4, 141.8, 128.4, 128.4, 125.9, 71.4, 65.5, 35.4, 28.2, 27.6, 27.5, 8.9. HRMS (ESI-TOF) calculated for $C_{14}H_{21}O_3$ $[M + H]^+$, 237.1491; observed, 237.1494.

5-Phenylpentyl 2-Hydroxybutyrate, 38. 38 was prepared according to method B, using 5-phenylpentan-1-ol to provide 5-phenylpentyl 2-hydroxybutyrate (220 mg, 88% yield). 1H NMR (500 MHz, $CDCl_3$) δ 7.29–7.11 (m, 2H), 7.19–7.12 (m, 3H), 4.22–4.07 (m, 3H), 2.71 (d, J = 5.7 Hz, 1H), 2.60 (t, J = 7.7 Hz, 2H), 1.84–1.76 (m, 1H), 1.71–1.58 (m, 5H), 1.43–1.33 (m, 2H), 0.93 (t, J = 7.4 Hz, 3H). ^{13}C NMR (126 MHz, $CDCl_3$) δ 175.6, 142.4, 128.6, 128.5, 126.0, 71.5, 65.8, 35.9, 31.2, 28.6, 27.7, 25.6, 9.1. HRMS (ESI-TOF) calculated for $C_{15}H_{23}O_3$ $[M + H]^+$, 251.1647; observed, 251.1655.

3-Cyclohexylpropyl 2-Hydroxybutyrate, 39. 39 was prepared according to method B, using 3-cyclohexyl-1-propanol to provide 3-cyclohexylpropyl 2-hydroxybutyrate (218 mg, 96% yield). 1H NMR (500 MHz, $CDCl_3$) δ 4.21–4.08 (m, 3H), 2.72 (s, 1H), 1.87–1.77 (m, 1H), 1.73–1.58 (m, 8H), 1.25–1.05 (m, 6H), 0.94 (t, J = 7.4 Hz, 3H), 0.90–0.78 (m, 2H). ^{13}C NMR (126 MHz, $CDCl_3$) δ 175.6, 71.6, 66.3, 37.5, 33.6, 33.5, 27.7, 26.8, 26.5, 26.2, 9.1. HRMS (ESI-TOF) calculated for $C_{13}H_{25}O_3$ $[M + H]^+$, 229.1804; observed, 229.1809.

4-Cyclohexylbutyl 2-Hydroxybutyrate, 40. 40 was prepared according to method B, using 4-cyclohexyl-1-butanol to provide 4-cyclohexylbutyl 2-hydroxybutyrate (225 mg, 93% yield). 1H NMR (500 MHz, $CDCl_3$) δ 4.22–4.09 (m, 3H), 2.78 (s, 1H), 1.87–1.76 (m, 1H), 1.70–1.56 (m, 8H), 1.37–1.28 (m, 2H), 1.24–1.03 (m, 6H), 0.94 (t, J = 7.4 Hz, 3H), 0.89–0.76 (m, 2H). ^{13}C NMR (126 MHz, $CDCl_3$) δ 175.6, 71.5, 66.0, 37.7, 37.2, 33.5, 29.0, 27.7, 26.9, 26.6, 23.2, 9.1. HRMS (ESI-TOF) calculated for $C_{14}H_{27}O_3$ $[M + H]^+$, 243.1960; observed, 243.1962.

5-Cyclohexylpentyl 2-Hydroxybutyrate, 41. 41 was prepared according to method B, using 5-cyclohexyl-1-butanol to provide 5-cyclohexylpentyl 2-hydroxybutyrate (151 mg, 59% yield). 1H NMR (500 MHz, $CDCl_3$) δ 4.21–4.10 (m, 3H), 2.73 (d, J = 5.7 Hz, 1H), 1.87–1.76 (m, 1H), 1.70–1.57 (m, 8H), 1.35–1.25 (m, 4H), 1.23–1.06 (m, 6H), 0.94 (t, J = 7.4 Hz, 3H), 0.88–0.76 (m, 2H). ^{13}C NMR (126 MHz, $CDCl_3$) δ 175.6, 71.5, 66.0, 37.8, 37.5, 33.6, 28.8, 27.7, 26.9, 26.6, 26.6, 26.3, 9.1. HRMS (ESI-TOF) calculated for $C_{15}H_{29}O_3$ $[M + H]^+$, 257.2117; observed, 257.2120.

1-(*p*-Butylphenyl)methyl 2-Hydroxybutyrate, 42. 42 was prepared according to method B, using (4-butylphenyl)methanol to provide 1-(*p*-butylphenyl)methyl 2-hydroxybutyrate (193 mg, 74% yield). 1H NMR (500 MHz, $CDCl_3$) δ 7.25 (d, J = 7.1 Hz, 2H), 7.17 (d, J = 8.0 Hz, 2H), 5.16 (s, 2H), 4.17 (dd, J = 6.7, 4.3 Hz, 1H), 2.59 (dd, J = 7.8, 7.8 Hz, 2H), 1.88–1.78 (m, 1H), 1.72–1.62 (m, 1H), 1.61–1.52 (m, 2H), 1.38–1.28 (m, 2H), 0.91 (t, J = 7.4 Hz, 3H), 0.90 (t, J = 7.3 Hz, 3H). ^{13}C NMR (126 MHz, $CDCl_3$) δ 175.4, 143.7, 132.5, 128.9, 128.7, 71.6, 67.6, 35.6, 33.8, 27.7, 22.5, 14.2, 9.1. HRMS (ESI-TOF) calculated for $C_{15}H_{22}O_3Na$ $[M + Na]^+$, 237.1466; observed, 273.14715.

1-(*m*-Butylphenyl)methyl 2-Hydroxybutyrate, 43. 43 was prepared according to method B, using (3-butylphenyl)methanol to provide 1-(*m*-butylphenyl)methyl 2-hydroxybutyrate (29 mg, 47%

yield). ^1H NMR (500 MHz, CDCl_3) δ 7.29–7.22 (m, 1H), 7.18–7.12 (m, 3H), 5.19 (A of AB, $J = 12.1$ Hz, 1H), 5.15 (B of AB, $J = 12.1$ Hz, 1H), 4.19 (dd, $J = 10.8$, 5.9 Hz, 1H), 2.72 (d, $J = 5.8$ Hz, 1H), 2.60 (dd, $J = 7.7$, 7.7 Hz, 2H), 1.89–1.78 (m, 1H), 1.73–1.62 (m, 1H), 1.61–1.51 (m, 2H), 1.39–1.28 (m, 2H), 0.95–0.87 (m, 6H). ^{13}C NMR (126 MHz, CDCl_3) δ 175.4, 143.7, 135.2, 128.9, 128.8, 128.7, 125.8, 71.6, 67.7, 35.7, 33.8, 27.7, 22.6, 14.2, 9.1. HRMS (ESI-TOF) calculated for $\text{C}_{15}\text{H}_{22}\text{O}_3\text{Na}$ [$\text{M} + \text{Na}$] $^+$, 273.1467; observed, 273.1478.

1-(*o*-Butylphenyl)methyl 2-Hydroxybutyrate, 44. 44 was prepared according to method B, using (2-butylphenyl)methanol to provide 1-(*o*-butylphenyl)methyl 2-hydroxybutyrate (55 mg, 40% yield). ^1H NMR (500 MHz, CDCl_3) δ 7.33–7.26 (m, 2H), 7.22–7.16 (m, 2H), 5.23 (s, 2H), 4.17 (dd, $J = 10.6$, 6.1 Hz, 1H), 2.72 (d, $J = 5.7$ Hz, 1H), 2.63 (dd, $J = 7.8$, 7.8 Hz, 2H), 1.88–1.78 (m, 1H), 1.72–1.62 (m, 1H), 1.59–1.50 (m, 2H), 1.42–1.33 (m, 2H), 0.92 (t, $J = 7.4$ Hz, 6H). ^{13}C NMR (126 MHz, CDCl_3) δ 175.4, 142.1, 132.7, 130.1, 129.8, 129.2, 126.3, 71.6, 65.7, 33.7, 32.5, 27.7, 23.0, 14.2, 9.1. HRMS (ESI-TOF) calculated for $\text{C}_{15}\text{H}_{22}\text{O}_3\text{Na}$ [$\text{M} + \text{Na}$] $^+$, 273.1467; observed, 273.1465.

1-(*p*-Pentylphenyl)methyl 2-Hydroxybutyrate, 45. was prepared according to method B, using (4-pentylphenyl)methanol to provide 1-(*p*-pentylphenyl)methyl 2-hydroxybutyrate (124 mg, 73% yield). ^1H NMR (500 MHz, CDCl_3) δ 7.25 (d, $J = 7.0$ Hz, 2H), 7.16 (d, $J = 8.0$ Hz, 2H), 5.16 (s, 2H), 4.17 (dd, $J = 10.8$, 6.0 Hz, 1H), 2.72 (d, $J = 5.7$ Hz, 1H), 2.58 (dd, $J = 7.7$ Hz, 2H), 1.87–1.77 (m, 1H), 1.72–1.62 (m, 1H), 1.62–1.54 (m, 2H), 1.35–1.25 (m, 4H), 0.91 (t, $J = 7.4$ Hz, 3H), 0.86 (t, $J = 6.9$ Hz, 3H). ^{13}C NMR (126 MHz, CDCl_3) δ 175.4, 143.8, 132.5, 128.9, 128.7, 71.6, 67.6, 35.9, 31.7, 31.3, 27.7, 22.7, 14.3, 9.1. HRMS (ESI-TOF) calculated for $\text{C}_{16}\text{H}_{24}\text{O}_3\text{Na}$ [$\text{M} + \text{Na}$] $^+$, 287.1623; observed, 287.1631.

1-(*m*-Pentylphenyl)methyl 2-Hydroxybutyrate, 46. 46 was prepared according to method B, using (3-pentylphenyl)methanol to provide 1-(*m*-pentylphenyl)methyl 2-hydroxybutyrate (170 mg, 81% yield). ^1H NMR (500 MHz, CDCl_3) δ 7.31–7.22 (m, 1H), 7.19–7.10 (m, 3H), 5.19 (A of AB, $J = 12.1$ Hz, 1H), 5.16 (B of AB, $J = 12.1$ Hz, 1H), 4.19 (dd, $J = 10.6$, 6.1 Hz, 1H), 2.72 (d, $J = 5.7$ Hz, 1H), 2.59 (dd, $J = 7.7$, 7.7 Hz, 2H), 1.89–1.78 (m, 1H), 1.74–1.64 (m, 1H), 1.64–1.53 (m, 2H), 1.37–1.24 (m, 4H), 0.92 (t, $J = 7.4$ Hz, 3H), 0.87 (t, $J = 6.8$ Hz, 3H). ^{13}C NMR (126 MHz, CDCl_3) δ 175.4, 143.7, 135.2, 128.9, 128.8, 128.6, 125.9, 71.6, 67.7, 36.0, 31.7, 31.4, 27.7, 22.7, 14.3, 9.1. HRMS (ESI-TOF) calculated for $\text{C}_{16}\text{H}_{24}\text{O}_3\text{Na}$ [$\text{M} + \text{Na}$] $^+$, 287.1623; observed, 287.1631.

3-(*p*-Ethylphenyl)propyl 2-Hydroxybutyrate, 47. 47 was prepared according to method B, using 3-(4-ethylphenyl)propan-1-ol to provide 3-(*p*-ethylphenyl)propyl 2-hydroxybutyrate (39 mg, 86% yield). ^1H NMR (500 MHz, CDCl_3) δ 7.11 (d, $J = 7.8$ Hz, 2H), 7.07 (d, $J = 7.8$ Hz, 2H), 4.24–4.10 (m, 3H), 2.70 (d, $J = 5.6$ Hz, 1H), 2.68–2.55 (m, 4H), 2.01–1.91 (m, 2H), 1.87–1.77 (m, 1H), 1.73–1.61 (m, 1H), 1.20 (t, $J = 7.6$ Hz, 3H), 0.95 (t, $J = 7.4$ Hz, 3H). ^{13}C NMR (126 MHz, CDCl_3) δ 175.5, 148.3, 138.2, 128.5, 128.2, 71.5, 65.2, 31.8, 30.4, 28.6, 27.7, 15.9, 9.2. HRMS (ESI-TOF) calculated for $\text{C}_{15}\text{H}_{23}\text{O}_3$ [$\text{M} + \text{H}$] $^+$, 251.1647; observed, 251.1660.

3-(*m*-Ethylphenyl)propyl 2-Hydroxybutyrate, 48. 48 was prepared according to method B, using 3-(3-ethylphenyl)propan-1-ol to provide 3-(*m*-ethylphenyl)propyl 2-hydroxybutyrate (231 mg, 92% yield). ^1H NMR (500 MHz, CDCl_3) δ 7.19 (t, $J = 7.5$ Hz, 1H), 7.03 (d, $J = 7.5$ Hz, 1H), 7.01–6.95 (m, 2H), 4.23–4.11 (m, 3H), 2.70 (d, $J = 5.7$ Hz, 1H), 2.68–2.57 (m, 4H), 2.03–1.93 (m, 2H), 1.89–1.78 (m, 1H), 1.72–1.62 (m, 1H), 1.21 (t, $J = 7.6$ Hz, 3H), 0.96 (t, $J = 7.4$ Hz, 3H). ^{13}C NMR (126 MHz, CDCl_3) δ 175.5, 144.7, 141.0, 128.7, 128.2, 125.9, 125.8, 71.6, 65.3, 32.3, 30.4, 29.0, 27.7, 15.8, 9.2. HRMS (ESI-TOF) calculated for $\text{C}_{15}\text{H}_{23}\text{O}_3$ [$\text{M} + \text{H}$] $^+$, 251.1647; observed, 251.1653.

3-(*o*-Ethylphenyl)propyl 2-Hydroxybutyrate, 49. 49 was prepared according to method B, using 3-(2-ethylphenyl)propan-1-ol to provide 3-(*o*-ethylphenyl)propyl 2-hydroxybutyrate (37 mg, 74% yield). ^1H NMR (500 MHz, CDCl_3) δ 7.19–7.09 (m, 4H), 4.30–4.07 (m, 4H), 2.76–2.58 (m, 4H), 1.99–1.90 (m, 2H), 1.89–1.78 (m, 1H), 1.73–1.63 (m, 1H), 1.20 (t, $J = 7.6$ Hz, 3H), 0.97 (t, $J = 7.4$ Hz, 3H). ^{13}C NMR (126 MHz, CDCl_3) δ 175.5, 142.1, 138.6, 129.3, 128.8,

126.7, 126.2, 71.6, 65.5, 30.1, 29.0, 27.7, 25.7, 15.6, 9.2. HRMS (ESI-TOF) calculated for $\text{C}_{15}\text{H}_{23}\text{O}_3$ [$\text{M} + \text{H}$] $^+$, 251.1647; observed, 251.1652.

***Vibrio cholerae* Agonism Bioassay.** Reporter strain MM920 (*V. cholerae* ΔcqsA ΔluxQ carrying pBB1 cosmid, which contains the *V. harveyi luxCDABE* luciferase operon) was used to assay agonist activity of each synthetic compound. This strain was grown in LB medium containing 10 $\mu\text{g}/\text{mL}$ tetracycline at 30 $^\circ\text{C}$ for >16 h and diluted 20-fold with the same medium. An amount of 2 μL of each synthetic compound dissolved in DMSO in various concentrations was added to 200 μL of the diluted reporter strain in triplicate in a 96-well plate. Bioluminescence and OD_{600} were measured in a PerkinElmer EnVision multilabel reader following a 4 h incubation at 30 $^\circ\text{C}$ with shaking. DMSO was used as the negative control.

***CqsS* C170Y and *CqsS* C170A mutants.** The *cqsS*^{C170Y} and *cqsS*^{C170A} alter the *Vibrio cholerae* *CqsS* receptor specificity to CAI-1 type ligands.^{8,13} To introduce these mutations to the genome of *Vibrio cholerae*, these two *cqsS* alleles were first cloned into the suicide vector pKAS32,²⁶ resulting in plasmids WN1957 (C170Y) and WN1961 (C170A), respectively. These two *cqsS* mutations were subsequently introduced into the genome of the *V. cholerae* strain WN1170 (ΔcqsA ΔluxQ) as described previously, resulting in WN1977 (ΔcqsA ΔluxQ *cqsS*^{C170Y}) and WN1982 (ΔcqsA ΔluxQ *cqsS*^{C170A}). The presence of the desired *cqsS* mutation was confirmed by sequencing. The *luxCDABE* operon from *Vibrio harveyi* carried on cosmid pBB1 was introduced into WN1977 and WN1982 by conjugation, yielding strain WN1989 and WN1994, respectively. Quorum-sensing dependent response from these *V. cholerae* strains was monitored by measuring bioluminescence in the presence of different ligands as described above.

Pharmacophore Modeling. Pharmacophore model generation was carried out using the software Ligand Scout. Ligand Scout, version 3.03b (inteligand.com), was used.^{18–20} The “training set” consisting of eight CAI-1 ester analogues that we had identified during our SAR studies. The compounds selected all displayed EC_{50} values of less than 0.2 μM and were capable of activating greater than 92% of the maximal quorum sensing response. A ligand-based pharmacophore was generated for the selected data. For pharmacophore generation, the sdf files of the data set, all as the (*S*)-stereoisomer, were provided as an input. The sdf files of the data set were obtained from ChemDraw Ultra using iLabel for file conversion. The sdf files were imported into Ligand Scout, and an unbiased pharmacophore model was generated using the default “BEST” settings, generating 500 unique conformers of each of the ligands and aligning each pharmacophore conformer to provide 10 best fit models that served as the pharmacophore model. Subsequent modeling of inactive analogues (“test set” compounds) was achieved using the pharmacophore model generated above and including a series of analogues displaying lower biological activity as “test set” analogues.

■ ASSOCIATED CONTENT

Supporting Information

Details of compound synthesis and spectral data (^1H NMR and ^{13}C NMR) for all compounds; primary bioassay data; pharmacophore modeling. This material is available free of charge via the Internet at <http://pubs.acs.org>.

■ AUTHOR INFORMATION

Corresponding Author

*Phone: 609 9333789. E-mail: mfshack@princeton.edu.

Present Addresses

¹Department of Chemistry and Biochemistry, Rowan University, Glassboro, NJ 08028, USA.

²Department of Molecular Biology and Microbiology, Tufts University School of Medicine, Boston, MA 02111, USA.

Notes

The authors declare no competing financial interest.

■ ACKNOWLEDGMENTS

The authors acknowledge Lotus Separations, LLC (Christina Kraml), for essential contributions to compound purification and enantiomer resolution. This work was supported by the Howard Hughes Medical Institute, the National Institutes of Health Grant 5R01AI054442, the National Science Foundation Grant MCB-0343821 to B.L.B., and an NIH Postdoctoral Fellowship GM082061 to W.-L.N.

■ ABBREVIATIONS USED

CAI-1, (S)-3-hydroxytridecan-4-one; Ea-CAI-1, 3-aminotridec-2-en-4-one; Ph-CAI-1, 1-hydroxy-1-phenylundecan-2-one; C8-CAI-1, (S)-3-hydroxyundecan-4-one

■ REFERENCES

- (1) Miller, M. B.; Bassler, B. L. Quorum sensing in bacteria. *Annu. Rev. Microbiol.* **2001**, *55*, 165–199.
- (2) Galloway, W. R. J. D.; Hodgkinson, J. T.; Bowden, S. D.; Welch, M.; Spring, D. R. Quorum sensing in Gram-negative bacteria: small-molecule modulation of AHL and AI-2 quorum sensing pathways. *Chem. Rev.* **2011**, *111*, 28–67.
- (3) Rasko, D. A.; Sperandio, V. Anti-virulence strategies to combat bacteria-mediated disease. *Nat. Rev. Drug Discovery* **2010**, *9*, 117–128.
- (4) Hentzer, M.; Givskov, M. Pharmacological inhibition of quorum sensing for the treatment of chronic bacterial infections. *J. Clin. Invest.* **2003**, *112*, 1300–1307.
- (5) Cegelski, L.; Marshall, G. R.; Eldridge, G. R.; Hultgren, S. J. The biology and future prospects of antivirulence therapies. *Nat. Rev. Microbiol.* **2008**, *6*, 17–27.
- (6) Ng, W. L.; Bassler, B. L. Bacterial quorum-sensing network architectures. *Annu. Rev. Genet.* **2009**, *43*, 197–222.
- (7) Higgins, D. A.; Pomianek, M. E.; Kraml, C. M.; Taylor, R. K.; Semmelhack, M. F.; Bassler, B. L. The major *Vibrio cholerae* autoinducer and its role in virulence factor production. *Nature* **2007**, *450*, 883–886.
- (8) Ng, W.-L.; Perez, L. J.; Wei, Y.; Kraml, C.; Semmelhack, M. F.; Bassler, B. L. Signal production and detection specificity in *Vibrio* CqsA/CqsS quorum-sensing systems. *Mol. Microbiol.* **2011**, *79*, 1407–1417.
- (9) Wei, Y.; Perez, L. J.; Ng, W.-L.; Semmelhack, M. F.; Bassler, B. L. Mechanism of *Vibrio cholerae* autoinducer-1 biosynthesis. *ACS Chem. Biol.* **2011**, *6*, 356–365.
- (10) Zhu, J.; Mekalanos, J. J. Quorum sensing-dependent biofilms enhance colonization in *Vibrio cholerae*. *Dev. Cell* **2003**, *5*, 647–656.
- (11) Spirig, T.; Taden, A.; Kiefer, P.; Buchrieser, C.; Vorholt, J. A.; Hilbi, H. The *Legionella* autoinducer synthase LqsA produces an alpha-hydroxyketone signaling molecule. *J. Biol. Chem.* **2008**, *283*, 18113–18123.
- (12) Bolitho, M. E.; Perez, L. J.; Koch, M. J.; Ng, W.-L.; Bassler, B. L.; Semmelhack, M. F. Small molecule probes of the receptor binding site in the *Vibrio cholerae* CAI-1 quorum sensing circuit. *Bioorg. Med. Chem.* **2011**, *19*, 6906–6918.
- (13) Ng, W.-L.; Wei, Y.; Perez, L. J.; Cong, J.; Long, T.; Koch, M.; Semmelhack, M. F.; Wingreen, N. S.; Bassler, B. L. Probing bacterial transmembrane histidine kinase receptor–ligand interactions with natural and synthetic molecules. *Proc. Natl. Acad. Sci. U.S.A.* **2010**, *107*, 5575–5580.
- (14) Miller, M. B.; Skorupski, K.; Lenz, D. H.; Taylor, R. K.; Bassler, B. L. Parallel quorum sensing systems converge to regulate virulence in *Vibrio cholerae*. *Cell* **2002**, *110*, 303–314.
- (15) Grasa, G. A.; Kissling, R. M.; Nolan, S. P. N-Heterocyclic carbenes as versatile nucleophilic catalysts for transesterification/acylation reactions. *Org. Lett.* **2002**, *4*, 3583–3586.
- (16) Grasa, G. A.; Guveli, T.; Singh, R.; Nolan, S. P. Efficient transesterification/acylation reactions mediated by N-heterocyclic carbene catalysts. *J. Org. Chem.* **2003**, *68*, 2812–2819.
- (17) Singh, R.; Kissling, R. M.; Letellier, M. A.; Nolan, S. P. Transesterification/acylation of secondary alcohols mediated by N-heterocyclic carbene catalysts. *J. Org. Chem.* **2004**, *69*, 209–212.
- (18) Wolber, G.; Langer, T. LigandScout: 3-d pharmacophores derived from protein-bound ligands and their use as virtual screening filters. *J. Chem. Inf. Model.* **2005**, *45*, 160–169.
- (19) Wolber, G.; Dornhofer, A. A.; Langer, T. Efficient overlay of small organic molecules using 3D pharmacophores. *J. Comput.-Aided Mol. Des.* **2006**, *20*, 773–788.
- (20) Yang, S.-Y. Pharmacophore modeling and applications in drug discovery: challenges and recent advances. *Drug Discovery Today* **2010**, *15*, 444–450.
- (21) Meanwell, N. A. Synopsis of some recent tactical application of bioisosteres in drug design. *J. Med. Chem.* **2011**, *54*, 2529–2591.
- (22) Choi, H.; Mascuch, S. J.; Villa, F. A.; Byrum, T.; Teasdale, M. E.; Smith, J. E.; Preskitt, L. B.; Rowley, D. C.; Gerwick, L.; Gerwick, W. H.; Honaucins, A.-C. Potent inhibitors of inflammation and bacterial quorum sensing: synthetic derivatives and structure–activity relationships. *Chem. Biol.* **2012**, *19*, 589–598.
- (23) Frezza, M.; Souleire, L.; Balestrino, D.; Gohar, M.; Deshayes, C.; Queneau, Y.; Forestier, C.; Doutheau, A. Ac-2-DPD, the bis-(O)-acetylated derivative of 4,5-dihydroxy-2,3-pentanedione (DPD) is a convenient stable precursor of bacterial quorum sensing autoinducer AI-2. *Bioorg. Med. Chem. Lett.* **2007**, *17*, 1428–1431.
- (24) Guo, M.; Gamby, S.; Nakayama, S.; Smith, J.; Sintim, H. O. A pro-drug approach for selective modulation of AI-2-mediated bacterial cell-to-cell communication. *Sensors* **2012**, *12*, 3762–3772.
- (25) Moore, C. G.; Murphy, P. J.; Williams, H. L.; McGown, A. T.; Smith, N. K. Synthetic studies towards ptilomycin A: total synthesis of crambescidin 359. *Tetrahedron* **2007**, *63*, 11771–11780.
- (26) Skorupski, K.; Taylor, R. K. Positive selection vectors for allelic exchange. *Gene* **1996**, *169*, 47–52.